NORSAR

ROYAL NORWEGIAN COUNCIL FOR SCIENTIFIC AND INDUSTRIAL RESEARCH

Norsar Technical Report No. 1/81

DYNAMIC RAY-TRACING IN COMPLEX THREE-DIMENSIONAL GEOLOGICAL MODELS

by
Jon Erik Reinhardsen

August 1981

NORSAR Contribution No. 305

DYNAMIC RAY-TRACING
IN COMPLEX THREE-DIMENSIONAL GEOLOGICAL MODELS

A thesis in applied mathematics

by

Jon Erik Reinhardsen

University of Bergen
August 1981

ACKNOWLEDGEMENTS

This work has been carried out at the data processing center of NTNF/ NORSAR. I would like to express my sincere thanks to the entire NORSAR staff whose helpful advice greatly facilitated this task. Special thanks are directed to H. Gjøystdal and S. Mykkeltveit for their valuable advice and encouragement which have greatly contributed to the completion of this thesis. Thanks are also due to E.S. Husebye for stimulating comments during the thesis work and to J. Fyen for his assistance on programming problems, on the bit level. I would also like to thank G. Berge as my adviser at the University of Bergen.

Kjeller, August 1981

Jon Erik Reinhardsen

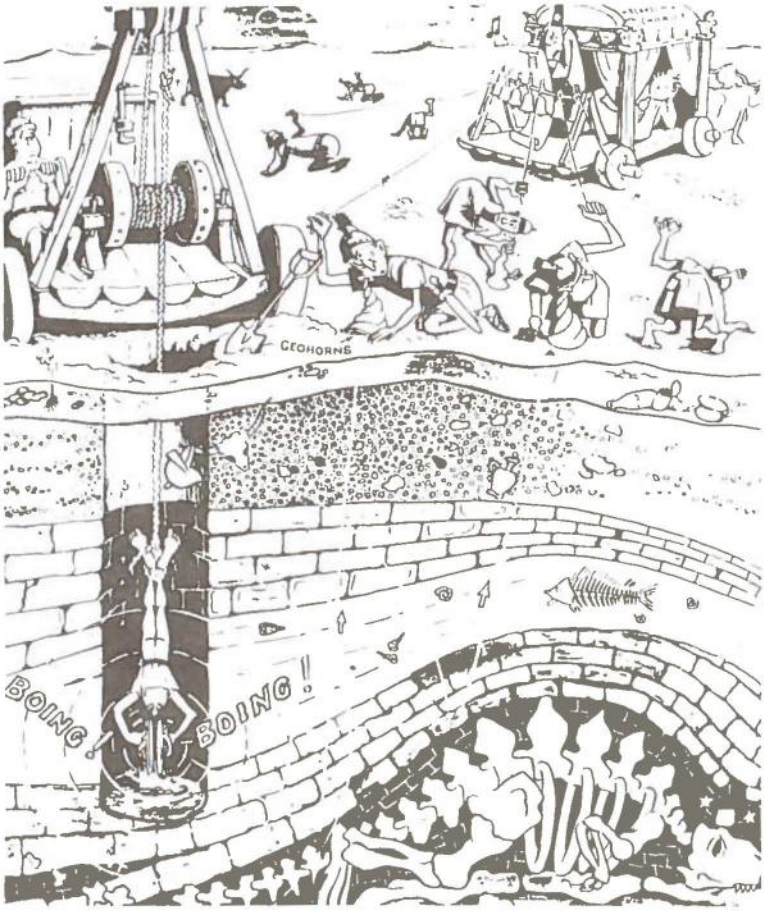
GEOHORNS
BOING!
BOING!

TABLE OF CONTENTS

1. INTRODUCTION

1.1 General Background

The use of seismic signals for studying subsurface structures of the earth has become an important tool in the field of oil exploration. In reflection seismology such methods are used to find discontinuities in the elastic properties of rocks by detecting and analyzing the faint 'echoes' which return from these regions when a pulse of energy (usually a small explosion or a shot from an airgun) is released near the surface of the ground. Due to the elastic properties of the medium stresses will be propagated away from the source as elastic waves. The velocities with which these waves travel depend on the elastic parameters and density of the rock. Since these parameters are different for different kinds of rocks, stresses will propagate with different speeds. At interfaces where the velocities change abruptly, part of the energy will be reflected, and thus part of the wave field will appear at the ground surface, where it can be recorded by sensitive instruments.

One of the main objectives of seismic processing techniques is to analyze the wave field recorded, and to extract information necessary to obtain a certain reconstruction of the subsurface geological structure.

The first efforts made in order to construct geological models from observed seismic data were based on the assumptions of horizontal layers each of constant velocity. In such models the computation of travel paths and corresponding travel times of the wave field is very simple, and a unique solution of velocities and layer thicknesses can be found analytically from the reflection times.

The really interesting and challenging geological features, like oil-bearing strata, however, normally deviate largely from the simple layered models depicted above. In conformity with this, numerous works have emphasized on the problems of computing seismic travel times in models of varying complexity. Most of these works have dealt with one- and two-dimensional models only. However, particularly during the last 5 years there has been a growing interest in the more complex three-dimensional case, and this has created a new branch of modern geophysical research: the 3-D seismic modelling.

Simply stated, we may consider seismic modelling as an attempt to mathematically represent the complex process of propagating seismic waves through a 3-D earth. Due to the lack of knowledge of various model parameters and their effects on the seismic response, one is, of course, forced to make a number of simplifications and assumptions. The concept of seismic modelling can be divided into two separate parts:

- forward modelling, i.e., computing the seismic response from a given geological model, and
- inverse modelling, i.e., computing the model from a given seismic response.

Quite frequently, the forward problem has to be solved prior to the inverse one. This applies for example when the inversion process consists of an iterative solution of the forward problem, starting with a 'guess model' and updating the model at each iteration step until the computed response matches the observed one. Obviously, the application of such inversion schemes calls for the utmost care in the assessment of the uniqueness of the solution.

1.2 The Concept of Seismic Ray-tracing

A very useful concept in the area of seismic modelling is the concept of ray-tracing. Seismic rays, which are spatial curves everywhere perpendicular to the wavefronts (in isotropic media), represent a convenient tool for computing the travel time of the wave between specified points in the medium. The reason for this is that the ray path obeys a simple system of equations that can easily be solved analytically or numerically, depending upon the nature of the velocity variation in the medium. Ray-tracing is the process of constructing specified ray paths in a model with given seismic velocities and reflecting interfaces and thereby calculating travel time, travel distance, etc., along each of these ray paths.

Various algorithms for tracing seismic rays through restricted earth models have been reported in the geophysical literature. For example, Sattlegger (1965) dealt with a two-dimensional model consisting of a sequence of constant-velocity layers separated by plane, dipping interfaces. Sorrells et al (1971) considered three-dimensional models made up of plane interfaces with arbitrary strike and dip. In the early seventies Shah (1973) presented

a more general algorithm which allowed tracing rays through a 3-D model consisting of curved interfaces of more general nature and with layers of continuously varying velocity. During the following years numerous works were presented on the problem of performing ray-tracing in geological models of varying complexity. For references, see, for example, Hubral (1976), Julian and Gubbins (1977) and Hubral and Krey (1980). As mentioned before, the application of advanced ray-tracing techniques is also an implicit prerequisite for many methods of seismic modelling including the generation of synthetic seismic sections.

1.3 The NORSAR 3-D Seismic Modelling Project - General Description

All papers mentioned so far mainly deal with the calculation of travel times only. In order to compute the seismic response of a model (i.e., theoretical seismograms), we also need a procedure for amplitude calculation. A relatively extensive discussion of some of the methods for computing theoretical seismograms can be found in Cerveny et al (1978). Most of these methods cannot be used to compute theoretical seismograms for general laterally inhomogeneous media with curved interfaces. However, the so-called 'ray method' is capable of giving valuable results for these types of media, especially after introducing modifications to increase the accuracy in singular regions. The basic references here would be Cerveny et al (1977) and Cerveny and Hron (1980). The method is also viewed from a slightly different angle by Hubral (1979, 1980).

Gjøystdal (presently at NORSAR) has developed a ray-tracing program for calculating ray paths and corresponding travel times in very complex 3-D geological models (see Gjøystdal, 1979). One major limitation, however, was that the procedure only included constant and linearly varying velocity functions, i.e., velocities giving analytical ray paths (straight or circular, respectively) within each layer. The interfaces separating the layers were allowed to have any shape that could be represented by a number of bicubic splines. The program is well suited both for forward modelling and inversion studies (Gjøystdal and Ursin, 1981) and has served as a basis for the work presented in this thesis.

In 1980 NORSAR decided to extend the 3-D ray-tracing project in order to develop a complete program package for the construction of theoretical seismograms for complex 3-D models. Briefly stated, this rather comprehensive task has been planned to comprise the development of the following items:

- more general velocity functions
- amplitude calculations based on recently developed theories in dynamic ray-tracing
- special procedures to overcome problems in the vicinity of caustics, etc., i.e., regions where the standard dynamic ray theory breaks down
- shear wave calculations
- special procedures to include diffraction effects at faults, edges, etc., in the model
- special procedures to include head waves caused by critical refraction
- frequency dependent attenuation in the medium (frictional loss)
- source functions
- statistical models for seismic noise that may be added to the synthetic traces in order to simulate realistic field records
- modification of the records to simulate contributions from instrument response.

1.4 The Aim of the Thesis

The work presented by this thesis can be regarded as a subtask of the above-mentioned project. In order to keep the work within proper limits, it was defined to include a specific part of the subjects listed in section 1.3. Thus, the aim of the thesis can be stated as follows:

- to implement more general velocity variations in the model, and to extend the ray-tracing algorithms to handle such variations.
- to develop numerical algorithms for amplitude modelling, based on recently developed theories in dynamic ray-tracing
- to evaluate the numerical algorithms and errors involved
- to demonstrate the applicability of the algorithms in practice by presenting a number of numerical examples.

In the first sections of chapter 2 we review the theories developed by Cerveny and Hron (1980) and Cerveny et al (1977). We have chosen to include these sections since they serve as a basis for the numerical algorithms developed. For some restricted earth models we have found analytical solutions of the differential equations.

In chapter 3 we adapt and apply the theories developed in order to obtain a numerical procedure for the dynamic tracing in a general medium. We describe a well suited procedure to perform the numerical integration of the ray-tracing differential equations. We also discuss the problem of representing the interfaces and the velocity structures in the medium. Finally we discuss some numerical problems asssociated with finding the intersection point between ray and interface.

In the fourth chapter we evaluate the method both theoretically and numerically. We discuss the most severe restrictions in applying the theories and evaluate the numerical errors introduced.

Finally, in chapter 5 we apply the procedures developed to construct synthetic seismograms. This includes development of algorithms used to find the proper ray between given source and receiver.

In the thesis we have assumed the most basic terms in the field of ray tracing to be known. In the following the words 'synthetic seismograms' and 'theoretical seismograms' have the same meaning. By 'homogeneous layers' we mean layers with constant velocity and thus 'inhomogeneous layers' are layers where the velocity varies as a function of space coordinates. Note also the slight distinction between the words 'ray-tracing' and 'dynamic ray-tracing'. By the first concept we mean the tracing of rays including the calculation of travel times, while dynamic ray-tracing includes in addition the calculation of the wavefront matrix, the Jacobian determinant and the amplitude coefficient.

2. THEORY

In this chapter we present theories which we have found very suitable for a numerical implementation. Sections 2.1 to 2.8 and 2.12 are reviews of theory developed in Cerveny and Hron (1980) and Cerveny et al (1977). They are included to make clear the basic ideas and assumptions of the theoretical developments.

2.1 Basic System of Equations

We consider a generally inhomogeneous, perfectly elastic medium with properties described by Lamé coefficients λ,μ and volume density ρ, all of which are continuously differentiable functions of Cartesian coordinates x_i, $i=1,2,3$. Let u_i denote the components of the complex displacement vector $\underline{u}(x_i,t)$ and let σ_{ij} be the components of the stress tensor.

Using the Einstein summation rule, we get for the basic elastodynamic equation:

$$\rho\, u_{i,tt} = \sigma_{ij,j} \qquad i=1,2,3,\ j=1,2,3 \qquad (2.1)$$

where

$$u_{i,tt} = \frac{\partial^2 u_i}{\partial t^2}$$

and

$$\sigma_{ij,j} = \sum_{j=1}^{3} \frac{\partial \sigma_{ij}}{\partial x_j}$$

In the following we shall use the above notation for partial derivatives of tensors of any order with respect to coordinates. For the stress tensors in (2.1) we use Hooke's law for an isotropic medium written in the form

$$\sigma_{ij} = \lambda\, \delta_{ij} u_{k,k} + \mu(u_{i,j}+u_{j,i}) \qquad (2.2)$$

where δ_{ij} is the Kronecker delta.

After some manipulations, we may write (2.1) in the following form

$$\rho u_{i,tt} = (\lambda+\mu)u_{j,ij} + \mu u_{i,jj} + \lambda_{,i}u_{j,j} + \mu_{,j}(u_{i,j}+u_{j,i}) \qquad (2.3)$$

2.2 The Ray Method

We seek solutions of (2.3) in terms of nonanalytic functions along some moving surfaces called wave fronts. Generally, any wave front at a time t can be implicitly described by the equation

$$t = \tau(x_i) \tag{2.4}$$

We assume that the components of the displacement vector may be written in the form of a ray series

$$u_i(x_j,t) = \sum_{k=0}^{\infty} U_i^{(k)}(x_j)\, F_k[t-\tau(x_j)] \tag{2.5}$$

Functions F_k are, in general, complex functions of real argument ξ satisfying relations

$$F_k' \equiv \frac{dF_k(\xi)}{d\xi} = F_{k-1}(\xi) \tag{2.6}$$

$$\begin{aligned} F_k(\xi) &= f_k(\xi) + i\, g_k(\xi) \\ g_k(\xi) &= \pi^{-1} \int_{-\infty}^{\infty} f_k(x)(x-\xi)^{-1}\, dx \end{aligned} \tag{2.7}$$

with real and imaginary parts f_k and g_k constituting Hilbert pairs of functions. The expansion is thus consisting of a series of terms, each of which is one degree smoother at the wavefront than its predecessor.

The vectorial complex function $\underline{U^{(k)}}(x_j) = [U_1^{(k)}, U_2^{(k)}, U_3^{(k)}]$ is called a k-th amplitude coefficient in the ray series, and the scalar function $\tau(x_j)$ is called a phase function or eikonal.

Following Cerveny and Hron (1980), inserting (2.5) into (2.3) and applying (2.6) gives

$$F_{-2}\{N_i[\underline{U}^{(o)}]\}+F_{-1}\{N_i[\underline{U}^{(1)}]-M_i[\underline{U}^{(o)}]\} + \sum_{k=0}^{\infty} F_k\{N_i[\underline{U}^{(k+2)}]-M_i[\underline{U}^{(k+1)}]+L_i[U^{(k)}]\} = 0 \quad , \; i = 1,2,3 \tag{2.8}$$

where

$$N_i(\underline{U}^{(k)})=-\rho U_i^{(k)}+(\lambda+\mu)U_j^{(k)}\tau_{,i}\tau_{,j}+ +\mu U_i^{(k)}\tau_{,j}\tau_{,j} \tag{2.9}$$

$$M_i(\underline{U}^{(k)}) = (\lambda+\mu)[U_{j,i}^{(k)}\tau_{,j}+U_{j,j}^{(k)}\tau_{,i}+U_j^{(k)}\tau_{,ij}] + +\mu[2U_{i,j}^{(k)}\tau_{,j}+U_i^{(k)}\tau_{,jj}]+\lambda_{,i}U_j^{(k)}\tau_{,j} + +\mu_{,j}U_i^{(k)}\tau_{,j}+\mu_{,j}U_j^{(k)}\tau_{,i} \tag{2.10}$$

$$L_i(\underline{U}^{(k)}) = (\lambda+\mu)U_{j,ij}^{(k)}+\mu U_{i,jj}^{(k)}+\lambda_{,i}U_{j,j}^{(k)} + +\mu_{,j}U_{i,j}^{(k)}+\mu_{,j}U_{j,i}^{(k)} \quad , \; j = 1,2,3 \tag{2.11}$$

We want (2.8) to be satisfied identically and this leads to a new system of equations

$$N_i(\underline{U}^{(o)}) = 0 \tag{2.12}$$

$$N_i(\underline{U}^{(1)}) - M_i(\underline{U}^{(o)}) = 0 \tag{2.13}$$

$$N_i(\underline{U}^{(k)}) - M_i(\underline{U}^{(k-1)}) + L_i(\underline{U}^{(k-2)}) = 0, \quad k \geq 2 \tag{2.14}$$

This is the basic system of equations in the ray method and can be used for the determination of all amplitude coefficients $\underline{U}^{(k)}$, k=0,1,2,... as well as the phase function τ.

2.3 Eikonal Equations

We will now consider eq. (2.12)

$$\underline{N}(\underline{U}^{(o)}) = 0$$

A nontrivial solution requires that the determinant of the system be equal to zero.

$$\begin{vmatrix} -\rho+(\lambda+\mu)\tau_{,1}{}^2+\mu\tau_{,k}\tau_{,k} & (\lambda+\mu)\tau_{,1}\tau_{,2} & (\lambda+\mu)\tau_{,1}\tau_{,3} \\ (\lambda+\mu)\tau_{,1}\tau_{,2} & -\rho+(\lambda+\mu)\tau_{,2}{}^2+\mu\tau_{,k}\tau_{,k} & (\lambda+\mu)\tau_{,2}\tau_{,3} \\ (\lambda+\mu)\tau_{,1}\tau_{,3} & (\lambda+\mu)\tau_{,2}\tau_{,3} & -\rho+(\lambda+\mu)\tau_{,3}{}^2+\mu\tau_{,k}\tau_{,k} \end{vmatrix} = 0 \qquad (2.15)$$

If we denote

$$\alpha = \sqrt{\frac{\lambda+2\mu}{\rho}} \quad , \quad \beta = \sqrt{\frac{\mu}{\rho}} \qquad (2.16)$$

equation (2.15) reduces to

$$(\tau_{,k}\tau_{,k} - \frac{1}{\alpha^2})(\tau_{,k}\tau_{,k} - \frac{1}{\beta^2})^2 = 0 \qquad (2.17)$$

Thus, the system (2.12) has a nontrivial solution if and only if one of the following conditions is satisfied

$$\tau_{,k}\tau_{,k} = \frac{1}{\alpha^2} \qquad (2.18)$$

$$\tau_{,k}\tau_{,k} = \frac{1}{\beta^2} \qquad (2.19)$$

These are generally known as the eikonal equations. Corresponding waves are called compressional (P) or shear (S) waves, depending on whether equation (2.18) or (2.19) is satisfied.

The method of characteristic curves applied to the eikonal equations gives a system of six ordinary differential equations

$$\frac{dx_i}{d\tau} = v^2 p_i, \quad \frac{dp_i}{d\tau} = -v^{-1} \frac{\partial v}{\partial x_i} \qquad i=1,2,3 \tag{2.20}$$

where $p_i = \dfrac{\partial \tau}{\partial x_i}$ are the components of the slowness vector and v is the velocity of the wave ($v = \alpha$ for P waves, $v = \beta$ for S waves).

The characteristic curves of the eikonal equations represent rays (see Cerveny et al, 1977, for details).

2.4 Introducing a New Coordinate System

Before investigating higher order equations in the basic system we will introduce a new coordinate system. The most commonly used system has the basis $\underline{t},\underline{n},\underline{b}$, where the unit vectors $\underline{t},\underline{n},\underline{b}$ represent the tangent, normal and binormal to the ray, respectively. A more convenient system for the ray tracing procedure is suggested by Cerveny et al (1977) and Popov and Psencik (1978a,b).

The basis vectors of the latter system are defined by

$$\underline{t} = \frac{d\underline{r}}{ds}, \qquad \underline{e}_1 = \underline{n}\cos\theta - \underline{b}\sin\theta, \qquad \underline{e}_2 = \underline{n}\sin\theta + \underline{b}\cos\theta \tag{2.21}$$

with

$$\theta(s) = \int_{s_o}^{s} T(x)dx + \theta(s_o) \tag{2.22}$$

where the integral is taken along the ray and T(x) is the torsion of the ray.

The value of $\theta(s_o)$ in (2.22) can be chosen arbitrarily, but once it is specified, the values of $\theta(s)$, $\underline{e}_1(s)$ and $\underline{e}_2(s)$ are determined uniquely by (2.21) and (2.22) We will denote the system defined by the basis vectors

$\underline{t},\underline{e}_1,\underline{e}_2$, a ray-centered coordinate system. Let K denote the curvature of the ray. Direct application of the Frenet formulas $d\underline{n}/ds = T\underline{b} - K\underline{t}$ and $d\underline{b}/ds = -T\underline{n}$ reveals important properties of $\underline{e}_1$ and $\underline{e}_2$, namely,

$$\frac{d\underline{e}_1}{ds} = -K\underline{t}\cos\theta \ , \quad \frac{d\underline{e}_2}{ds} = -K\underline{t}\sin\theta \tag{2.23}$$

Let us select an arbitrary ray that will be called the central ray. If the ray-centered coordinate system $[s,q_1,q_2]$ with the basis vectors $\underline{t},\underline{e}_1,\underline{e}_2$ satisfying equations (2.21) to (2.23) is introduced for the ray, then q_1,q_2 represent length coordinates in the plane perpendicular to the central ray, s being the length of the central ray from some reference point on the ray. Thus, a position vector of any point at the vicinity of the central ray can be written as

$$\underline{r}(s,q_1,q_2) = \underline{r}(s,o,o) + q_1\underline{e}_1(s) + q_2\underline{e}_2(s)$$

It can be shown (Cerveny and Hron, 1980) that the ray-centered coordinate system is orthogonal and that

$$dr^2 = h^2ds^2 + dq_1^2 + dq_2^2 \tag{2.24}$$

where the scale factor h is given by

$$h = 1 - K(q_1\cos\theta + q_2\sin\theta) \tag{2.25}$$

and dr is the length of the infinitesimal vector $d\underline{r}$.

2.5 Transport Equations

We shall now investigate the higher order equations in the basic system, and we shall mainly be concerned with the amplitude coefficient $\underline{U}^{(k)}$ in the ray series. For signals satisfying our assumptions, P and S waves propagate independently in elastic media. (α and β are independent in the eikonal equations.) The amplitude coefficient $\underline{U}^{(k)}$ pertaining to different kinds of elastic waves (P or S) can therefore be studied separately.

In both cases we can write

$$\underline{U}^{(k)} = U_p^{(k)}\underline{t}+U_{s1}^{(k)}\underline{e}_1+U_{s2}^{(k)}\underline{e}_2 = \underline{U}_{\parallel}^{(k)} + \underline{U}_{\perp}^{(k)} \tag{2.26}$$

with two vector components

$$\underline{U}_{\parallel}^{(k)} = U_p^{(k)}\underline{t} , \quad \underline{U}_{\perp}^{(k)} = U_{s1}^{(k)}\underline{e}_1+U_{s2}^{(k)}\underline{e}_2 \tag{2.27}$$

indicating the polarization of the displacement in the direction parallel and perpendicular to the ray, respectively. For P waves we will call $\underline{U}^{(k)}{}_{\parallel}$ and $\underline{U}^{(k)}{}_{\perp}$ principal and additional components of the amplitude coefficient $\underline{U}^{(k)}$, respectively. In the other case, the S waves, the principal and additional components will be represented by $\underline{U}^{(k)}{}_{\perp}$ and $\underline{U}^{(k)}{}_{\parallel}$, respectively. The advantage of this resolution of $\underline{U}^{(k)}$ using (2.26) rests in a high degree of simplicity and symmetry of the final formulas.

Amplitude coefficient for P waves

Let us consider additional components for P waves $U_{s1}^{(k)}$ and $U_{s2}^{(k)}$ first. Multiplication of equation (2.9) by vectors $\underline{e}_1$ and $\underline{e}_2$ yields two scalar products

$$\begin{aligned} N_i(\underline{U}^{(k)})e_{1i} &= (-\rho+\mu\alpha^{-2})U_{s1}^{(k)}, \\ N_i(\underline{U}^{(k)})e_{2i} &= (-\rho+\mu\alpha^{-2})U_{s2}^{(k)} \end{aligned} \tag{2.28}$$

Taking the scalar products of equation (2.14) with $\underline{e}_1$ and $\underline{e}_2$ using (2.28) leads to the final expression for the additional components of P waves $U_{s1}^{(k)}$ and $U_{s2}^{(k)}$

$$\begin{aligned} U_{s1}^{(k)} &= (-\rho+\mu\alpha^{-2})^{-1}[M_i(\underline{U}^{(k-1)})-L_i(\underline{U}^{(k-2)})]e_{1i} \\ U_{s2}^{(k)} &= (-\rho+\mu\alpha^{-2})^{-1}[M_i(\underline{U}^{(k-1)})-L_i(\underline{U}^{(k-2)})]e_{2i} \end{aligned} \qquad k \geq 2 \tag{2.29}$$

Observe that (2.29) is valid for $k \geq 0$ if we define

$$\underline{U}^{(-1)} = \underline{U}^{(-2)} = 0$$

In vectorial notation we get

$$\underline{U}_{\perp}^{(k)} = (-\rho+\mu\alpha^{-2})^{-1}[\underline{M}_{\perp}(\underline{U}^{(k-1)})-\underline{L}_{\perp}(\underline{U}^{(k-2)})], \quad k > 0 \tag{2.30}$$

We observe that for k=0 the additional components for P waves vanish.

Let us now consider the principal component for P waves. First we take the scalar product of equation (2.14) with $\tau_{,i}$ (the gradient of the phase function τ). Since $N_i\tau_{,i}=0$ we get the following vector equation:

$$M_i(\underline{U}^{(k)})\tau_{,i} = L_i(\underline{U}^{(k-1)})\tau_{,i} \tag{2.31}$$

The linearity of the vector operator $\underline{M}$ gives

$$M_i(\underline{U}_{\parallel}^{(k)})\tau_{,i} = [L_i(\underline{U}^{(k-1)})-M_i(\underline{U}_{\perp}^{(k)})]\tau_{,i} \tag{2.32}$$

Here all the functions on the right side are known due to the recurrent character of the basic system (2.12-14) and equation (2.30).

Following Cerveny and Hron (1980) gives us

$$\frac{dU_p^{(k)}}{d\tau} + \tfrac{1}{2}U_p^{(k)}(\alpha^2\tau_{,jj} + \frac{d\ \ln(\rho\alpha^2)}{d\tau}) = g_o^{(k)}(\tau), \quad k=0,1,2,\ldots \tag{2.33}$$

with

$$g_o^{(k)}(\tau) = \frac{\alpha}{2\rho}[L_i(\underline{U}^{(k-1)})-M_i(\underline{U}_{\perp}^{(k)})]\tau_{,i}, \qquad k=0,1,2,\ldots \tag{2.34}$$

from which the principal components for P waves, $U_p^{(k)}$, is obtained.

Equation (2.33) is known in the literature as a transport equation.

Amplitude coefficients for S waves

As in the case of P waves we start with the additional component. Scalar multiplication of equation (2.14) by the vector $\underline{t}$ tangent to the ray gives

$$N_i(\underline{U}^{(k)})t_i = [M_i(\underline{U}^{(k-1)})-L_i(\underline{U}^{(k-2)})]t_i$$

where the left side can be written as

$$N_i(\underline{U}^{(k)})t_i = (\lambda+\mu)\beta^{-2}U_p^{(k)}$$

Hence we have

$$U_p^{(k)} = \frac{\beta^2}{\lambda+\mu}[M_i(\underline{U}^{(k-1)})-L_i(\underline{U}^{(k-2)})]t_i \qquad (2.35)$$

Again we observe that the additional component vanishes for k=0.

The derivation of differential equations for the principal components of S waves, $U_{s1}^{(k)}$ and $U_{s2}^{(k)}$, is similar to the way the principal component of P waves, $U_p^{(k)}$, was obtained. We observe that $N_i(\underline{U}^{(k)})\, e_{1i} = 0$ and $N_i(\underline{U}^{(k)})\, e_{2i} = 0$.

The scalar multiplication of (2.14) by $\underline{e}_1$ and $\underline{e}_2$ then gives

$$M_i(\underline{U}^{(k)})e_{1i} = L_i(\underline{U}^{(k-1)})e_{1i}, \quad M_i(\underline{U}^{(k)})e_{2i} = L_i(\underline{U}^{(k-1)})e_{2i} \qquad (2.36)$$

Using the linearity of $\underline{M}$ we get

$$\begin{aligned} M_i(\underline{U}_{\perp}^{(k)})e_{1i} &= [L_i(\underline{U}^{(k-1)})-M_i(\underline{U}_{\parallel}^{(k)})]e_{1i} \\ M_i(\underline{U}_{\perp}^{(k)})e_{2i} &= [L_i(\underline{U}^{(k-1)})-M_i(\underline{U}_{\parallel}^{(k)})]e_{2i} \end{aligned} \qquad (2.37)$$

Equations (2.37) are similar to equations (2.32).

Again following Cerveny and Hron (1980) leads to

$$\frac{dU_{s1}^{(k)}}{d\tau} + \tfrac{1}{2} U_{s1}^{(k)}(\beta^2\tau_{,ii} + \frac{d\ \ln(\rho\beta^2)}{d\tau}) = g_1^{(k)}(\tau) \tag{2.38}$$

The corresponding expression for $U_{s2}^{(k)}$ is

$$\frac{dU_{s2}^{(k)}}{d\tau} + \tfrac{1}{2} U_{s2}^{k}(\beta^2\tau_{,ii} + \frac{d\ \ln(\rho\beta^2)}{d\tau}) = g_2^{(k)}(\tau) \tag{2.39}$$

where

$$g_1^{(k)}(\tau) = (2\rho)^{-1}\ [L_i(\underline{U}^{(k-1)}) - M_i(\underline{U}_{\parallel}^{(k)})]\ e_{1i} \tag{2.40}$$

and

$$g_2^{(k)}(\tau) = (2\rho)^{-1}\ [L_i(\underline{U}^{(k-1)}) - M_i(\underline{U}_{\parallel}^{(k)})]\ e_{2i} \tag{2.41}$$

The decoupling of systems (2.38) and (2.39) is due to the proper choice of coordinate system $[s,q_1,q_2]$. This has been obtained independently by both Hubral (1979) and Cerveny and Hron (1980).

2.6 Solution of Transport Equations

Let $U^{(k)} = U_p^{(k)}$, $v = \alpha$, $g^{(k)} = g_o^{(k)}$ in the case of P waves and $U^{(k)} = U_{s1}^{(k)}$ (or $U^{(k)} = U_{s2}^{(k)}$), $v = \beta$, $g^{(k)} = g_1^{(k)}$, (or $g^{(k)} = g_2^{(k)}$) for S waves.

Then equations (2.33), (2.38) and (2.39) can be written in one simple form

$$\frac{dU^{(k)}}{d\tau} + \tfrac{1}{2} U^{(k)}(v^2\tau_{,ii} + \frac{d\ \ln(\rho v^2)}{d\tau}) = g^{(k)}(\tau) \tag{2.42}$$

Let J be the Jacobian of the transformation from Cartesian coordinates into ray coordinates $[s,\gamma_1,\gamma_2]$. Here the ray coordinates (ray parameters) γ_1 and γ_2 specify a particular ray, the position on which is characterized by the remaining coordinate s.

Realizing that

$$\tau_{,ii} = \frac{1}{Jv}\frac{d}{d\tau}\left(\frac{J}{v}\right) \tag{2.43}$$

(see Cerveny and Ravindra, 1971), we get for the solution of (2.42)

$$U^{(k)}(\tau) = \left[J(\tau)v(\tau)\rho(\tau)\right]^{-\frac{1}{2}} \tag{2.44}$$

$$\left\{\phi^{(k)}(\gamma_1,\gamma_2)+\int_{\tau_o}^{\tau}\left[J(\xi)v(\xi)\rho(\xi)\right]^{\frac{1}{2}}g^{(k)}(\xi)\,d\xi\right\}$$

The constant of integration $\phi^{(k)}(\gamma_1,\gamma_2)$ (or source function) is a function of ray parameters and depends on the mode of wave propagation. The integration is carried out along the ray.

Equation (2.44) can be written in an equivalent form

$$U^{(k)}(\tau) = U^{(k)}(\tau_o)\left[\frac{J(\tau_o)\rho(\tau_o)v(\tau_o)}{J(\tau)\rho(\tau)v(\tau)}\right]^{\frac{1}{2}} + \tag{2.45}$$

$$+\left[J(\tau)\rho(\tau)v(\tau)\right]^{-\frac{1}{2}}\int_{\tau_o}^{\tau}\left[J(\xi)v(\xi)\rho(\xi)\right]^{\frac{1}{2}}g^{(k)}(\xi)\,d\xi$$

provided that $U^{(k)}$ is known at some point on the ray corresponding to $\tau = \tau_o$. In the zero order approximation of the ray series (k=0) we have $g^{(o)} \equiv 0$ and (2.44-45) reduce to

$$U^{(o)}(\tau) = \phi^{(o)}(\gamma_1,\gamma_2)\left[J(\tau)v(\tau)\rho(\tau)\right]^{-\frac{1}{2}}$$

$$U^{(o)}(\tau) = U^{(o)}(\tau_o)\left[\frac{J(\tau_o)v(\tau_o)\rho(\tau_o)}{J(\tau)v(\tau)\rho(\tau)}\right]^{\frac{1}{2}} \tag{2.46}$$

2.7 Eikonal Equation in the Ray-centered Coordinate System

We now seek an expression for $J(\tau)$ along the ray. To get that we need a closer look at the eikonal equation. From (2.24) we can write

$$\nabla\tau = \frac{1}{h}\frac{\partial\tau}{\partial s}\underline{t} + \frac{\partial\tau}{\partial q_1}\underline{e}_1 + \frac{\partial\tau}{\partial q_2}\underline{e}_2 \tag{2.47}$$

For the eikonal equations we get

$$\nabla\tau\cdot\nabla\tau = \frac{1}{h^2}\tau_{,s}^{\,2} + \tau_{,1}^{\,2} + \tau_{,2}^{\,2} = \frac{1}{v^2} \tag{2.48}$$

where v represents the velocity of the wave, $\tau_{,s} = \partial\tau/\partial s$, $\tau_{,1} = \partial\tau/\partial q_1$, $\tau_{,2} = \partial\tau/\partial q_2$ and h is given by (2.25).

A more convenient expression of (2.48) is

$$\tau_{,s} = \frac{h}{v}\left[1-v^2(\tau_{,1}^{\,2}+\tau_{,2}^{\,2})\right]^{\frac{1}{2}} \tag{2.49}$$

We observe that (2.49) is equivalent to the Hamilton-Jacobi equation for the functional $\int_{M_o}^{M} v^{-1}dr$ with the length element given in equation (2.24). The corresponding Hamiltonian is

$$H(q_i,p_i) = -\frac{h}{v}\left[\,1-v^2(p_1^2+p_2^2)\right]^{\frac{1}{2}} \tag{2.50}$$

where q_i are generalized coordinates and p_i are generalized moments.

A Taylor expansion of the phase function $\tau(s,q_1,q_2)$ around the central ray up to the second order gives

$$\tau(s,q_1,q_2) \simeq \tau(s,0,0) + \tfrac{1}{2}\, q^T M q \tag{2.51}$$

with q^T denoting the transposed matrix of q and where

$$M = \begin{bmatrix} M_{11} & M_{12} \\ M_{12} & M_{22} \end{bmatrix}, \quad M_{ij} = \left.\frac{\partial^2 \tau(s,q_1,q_2)}{\partial q_i \partial q_j}\right|_{q_1=q_2=0}, \quad q = \begin{bmatrix} q_1 \\ q_2 \end{bmatrix} \tag{2.52}$$

For the derivatives we get

$$\tau_{,s} \simeq v^{-1} + \tfrac{1}{2}\, q^T M' q \tag{2.53}$$

$$\tau_{,1} \simeq M_{11}q_1 + M_{12}q_2 , \qquad \tau_{,2} \simeq M_{12}q_1 + M_{22}q_2 \tag{2.54}$$

where the prime denotes differentiation with respect to s. We now seek a Taylor expansion of (2.50) around the central ray up to the second order. This expansion is matched with (2.53) and we get the following two equations:

$$h = 1 + v^{-1}(q_1 v_{,1} + q_2 v_{,2}) \tag{2.55}$$

where

$$v_{,i} = \left.\frac{\partial v}{\partial q_i}\right|_{q_1=q_2=0}$$

and

$$H(q_1,q_2,\tau_{,1},\tau_{,2}) = -v^{-1} + \tfrac{1}{2}v(\tau_{,1}^2 + \tau_{,2}^2) + \tag{2.56}$$

$$+ \tfrac{1}{2}v^{-2}(v_{,11}q_1^2 + v_{,22}q_2^2 + 2v_{,12}q_1q_2)$$

where

$$v_{,ij} = \left.\frac{\partial^2 v}{\partial q_i \partial q_j}\right|_{q_1=q_2=0}$$

Equations (2.53), (2.54) and (2.56) together with (2.49) and (2.50) now give us the following equation:

$$\tfrac{1}{2}[M_{11}'+v(M_{11}^2+M_{12}^2)+v^{-2}v_{,11}]q_1^2 + \tag{2.57}$$

$$+ \tfrac{1}{2}[M_{22}'+v(M_{22}^2+M_{12}^2)+v^{-2}v_{,22}]q_2^2 +$$

$$+ [M_{12}'+vM_{12}(M_{11}+M_{22})+v^{-2}v_{,12}]q_1q_2 = 0$$

This is the eikonal equation written in ray-centered coordinates. From (2.57) it follows

$$\begin{aligned}
&\frac{dM_{11}}{ds} + v(M_{11}^2+M_{12}^2) = -v^{-2}v_{,11} \\
&\frac{dM_{22}}{ds} + v(M_{22}^2+M_{12}^2) = -v^{-2}v_{,22} \qquad (2.58) \\
&\frac{dM_{12}}{ds} + v(M_{11}+M_{22})M_{12} = -v^{-2}v_{,12}
\end{aligned}$$

or in matrix form

$$\frac{dM}{ds} + vM^2 = -v^{-2}V \tag{2.59}$$

where

$$V = \begin{bmatrix} v_{,11} & v_{,12} \\ v_{,12} & v_{,22} \end{bmatrix}$$

Equation (2.59) is a first order ordinary nonlinear differential equation of the Riccati type in the matrix form. In general this equation cannot be solved by elementary analytical methods. It can, of course, be solved numerically.

From Deschamps (1972), Lee (1975), and James (1976) we have the direct connection between M and the so-called curvature matrix of the wave front K by

$$M = \frac{1}{v} K \tag{2.60}$$

We point out that K is a 2x2 matrix and should not be confused with the K introduced in equation (2.23) which was the curvature of the ray path.

From (2.59) and (2.60) we get

$$v \frac{dK}{ds} - v_{,s} K + vK^2 = -V \tag{2.61}$$

Introducing $N=M^{-1}$ and $R=K^{-1}$ we get

$$\frac{dN}{ds} - v^{-2} NVN = vI \tag{2.62}$$

and

$$v \frac{dR}{ds} + v_{,s} R - RVR = vI \tag{2.63}$$

where I in both equations is the 2x2 identity matrix.

Using travel time τ as a parameter along the ray gives the following four equations instead of equations (2.59), (2.61), (2.62) and (2.63):

$$\frac{dM}{d\tau} + v^2 M^2 = -v^{-1} V \tag{2.64}$$

$$\frac{dK}{d\tau} - v^{-1} v_{,\tau} K + vK^2 = -V \tag{2.65}$$

$$\frac{dN}{d\tau} - v^{-1} NVN = v^2 I \tag{2.66}$$

$$\frac{dR}{d\tau} + v^{-1} v_{,\tau} R - RVR = vI \tag{2.67}$$

2.8 An Expression for J(τ) along the Central Ray

From equations (2.53) and (2.54) we get

$$\nabla^2\tau = \tau_{,ii} = \frac{\partial}{\partial s}\left(\frac{1}{v}\right) + M_{11} + M_{22} \tag{2.68}$$

evaluated on the central ray.

This equation enables us to write the solution of equation (2.43) as

$$J(\tau) = J(\tau_o)\exp\left\{\int_{\tau_o}^{\tau} v^2(M_{11}+M_{22})d\tau\right\} \tag{2.69}$$

If we denote the eignevalues of the matrix M as M_1 and M_2, we observe that $M_{11} + M_{22} = M_1 + M_2$.

Equation (2.69) in terms of the matrix K is written

$$J(\tau) = J(\tau)\exp\left\{\int_{\tau_o}^{\tau} v(K_{11}+K_{22})d\tau\right\} \tag{2.70}$$

2.9 Amplitude Calculations

In order to calculate the amplitude of the ray given by one of equations (2.46), it is generally necessary to perform a numerical solution of one of the Riccati equations (2.64-67) followed by a numerical integration of one of equations (2.69-70). In the next section we will show that an analytical expression for J(τ) can be found in a medium with constant velocity gradient.

2.10 Investigating the Case of Constant Velocity Gradient

The solution of the equations developed so far may be found analytically in some special cases. It is readily conceived that the straightforward application of an analytic formula is much faster than a numerical integration of a differential equation. Therefore it is of great importance for the practical use of the theory to find analytic solutions for models being as general as possible.

The ray-centered coordinates

Let us assume that the velocity gradient is a constant vector. Using (2.20) and $\underline{t} = v\underline{p}$ where $\underline{p}$ is the slowness vector, we get

$$\frac{d}{d\tau}\underline{t} = \frac{1}{v}\frac{dv}{d\tau}\underline{t} - \nabla v \tag{2.71}$$

We see that the change in $\underline{t}$ and henceforth the ray is confined to the plane defined by $\underline{t}(\tau_o)$ and ∇v, and hence both $\underline{t}$ and the ray are confined to the same plane. We also observe that the normal vector $\underline{n}$, which is proportional to $d\underline{t}/d\tau$ lies in the same plane.

The unit binormal $\underline{b}$ which is given as

$$\underline{b} = \underline{t} \times \underline{n} \tag{2.72}$$

is thus a constant vector normal to this plane. From one of the Frenet formulas we have

$$\frac{d\underline{b}}{ds} = -T\,\underline{n} = \underline{0} \tag{2.73}$$

which means that the torsion T of the ray is zero.

This argument does not hold in the two cases $\nabla v = \underline{0}$ and $\nabla v \parallel \underline{t}$. In these cases $d\underline{t}/d\tau = \underline{0}$ and thus $\underline{t}$ is a constant vector. The vector $\underline{n}$ is then arbitrarily given, but fixed, and thus by (2.72) and (2.73) we may conclude that the torsion is zero. This means, according to equations (2.21) and (2.22) that the ray-centered basis vectors remain at a fixed angle to the $\underline{t}$, $\underline{n}$, $\underline{b}$ vectors along the ray. The angle can be chosen arbitrarily at the initial point of the ray.

The dynamic ray-tracing system

In case of a constant velocity gradient it is obvious that

$$\frac{\partial v}{\partial q_i} = \nabla v \cdot \underline{e}_i \tag{2.74}$$

is independent of both q_1 and q_2. Hence the second derivative of v with respect to q_i vanishes.

$$): \quad \frac{\partial^2 v}{\partial q_i \partial q_j} = 0 \qquad \text{for } j=1,2, \quad i=1,2 \tag{2.75}$$

The last of equations (2.58) is in this case a homogeneous linear differential equation of the first order

$$\frac{dM_{12}}{d\tau} + v(M_{11} + M_{22})M_{12} = 0$$

with solution

$$M_{12}(\tau) = M_{12}(\tau_o)\exp-\{ \int_{\tau_o}^{\tau} v(M_{11}+M_{12})d\tau\} \tag{2.76}$$

From (2.76) we conclude that if M_{12} is zero at one point, $\tau=\tau_o$, of the ray in a certain layer with constant velocity gradient, then M_{12} is zero along the whole ray in that layer. Hence, starting in a layer with constant velocity gradient and choosing basis vectors $\underline{e}_1$ and $\underline{e}_2$ along the principal directions of wavefront curvature initially, will cause the basis vectors $\underline{e}_1$ and $\underline{e}_2$ to coincide with the prinicipal directions along the whole ray within that layer. Note that (2.76) is valid even if we just claim $v_{,12} = 0$ instead of (2.75).

If we now write equation (2.69) as

$$J(\tau) = J_1(\tau) \cdot J_2(\tau)$$

where

$$J_1(\tau) = J_1(\tau_o)\exp\{ \int_{\tau_o}^{\tau} v^2 M_{11} d\tau\} \ , \quad J_2(\tau) = J_2(\tau_o)\exp\{ \int_{\tau_o}^{\tau} v^2 M_{22} d\tau\} \tag{2.77}$$

we may, by a proper choice of $\underline{e}_1$ and $\underline{e}_2$ such that $M_{12}(\tau_o) = 0$, handle the components J_1 and J_2 separately.

This is due to the decoupling of the equations for the matrix M into two equations

$$\frac{dM_{11}}{d\tau} + v^2 M_{11}^2 = -v^{-1} v_{,11} = 0$$

and (2.78)

$$\frac{dM_{22}}{d\tau} + v^2 M_{22}^2 = -v^{-1} v_{,22} = 0$$

when $M_{12} = 0$.

We get similar equations for matrices K, N and R. For the first component in N we get

$$\frac{dN_{11}}{d\tau} = v^2 \tag{2.79}$$

with solution

$$N_{11}(\tau) = N_{11}(\tau_o) + \int_{\tau_o}^{\tau} v^2(t)\, dt \tag{2.80}$$

which in the system of principal curvatures, automatically gives

$$R_{11}(\tau) = \frac{1}{v(\tau)} N_{11}(\tau), \quad K_{11}(\tau) = R_{11}^{-1}(\tau), \quad M_{11}(\tau) = N_{11}^{-1}(\tau) \tag{2.81}$$

The treatment of the N_{22} component is similar.

In the case of constant velocity, equation (2.80) simply gives

$$N_{11}(\tau) = N_{11}(\tau_o) + v^2(\tau)(\tau-\tau_o) \tag{2.82}$$

which is what we should expect.

The main problem in calculating the Jacobian $J(\tau)$ has now been reduced to the numerical evaluation of three integrals. The first is the integral

$$\int_{\tau_o}^{\tau} v^2(t)\, dt$$

in equation (2.80).

The next integrals are

$$\int_{\tau_o}^{\tau} v^2 M_{ii}\, d\tau \qquad i=1,2$$

in equations (2.77).

We will now put some effort in finding the $N_{ii}(\tau)$, i=1,2 of equation (2.80) as an analytic function of τ. In other words we want to find an analytic expression for the first integral mentioned above. We may assume $\nabla v \neq \underline{0}$ since this case is solved in equation (2.82). Provided that ∇v is a constant vector, not parallel to $\underline{t}$, we get from Ursin (1981A)

$$\underline{r}(s) = \underline{r}(s_o)+\rho\left[\sin\frac{s-s_o}{\rho}\,\underline{t}(s_o)+(1-\cos\frac{s-s_o}{\rho})\underline{n}(s_o)\right] \tag{2.83}$$

where ρ is the radius of ray curvature given by

$$\rho = \frac{1}{|\nabla v \times \underline{p}|} = \frac{v(s)}{|\nabla v \times \underline{t(s)}|} = \text{const.} \quad \text{(according to Snell's law)} \tag{2.84}$$

and $\underline{r}(s)$ is the position vector ($\underline{r}(s) = (x_1(s), x_2(s), x_3(s))$ along the ray.

Expressing equation (2.80) in terms of distance along the ray, s, gives

$$N_{ii}(s) = N_{ii}(s_o) + \int_{s_o}^{s} v(s)ds \tag{2.85}$$

Now let

$$v(s) = v(\underline{r}(s)) = v(x_1, x_2, x_3) = a_o + \sum_{i=1}^{3} a_i x_i \tag{2.86}$$

According to equation (2.83) we get

$$v(s) = v(s_o)+\rho \sum_{i=1}^{3} a_i\left[t_i(s_o)\sin\frac{s-s_o}{\rho} + n_i(s_o)(1-\cos\frac{s-s_o}{\rho})\right] \qquad (2.87)$$

After integration is performed, N_{ii} is written as:

$$N_{ii}(s) = N_{ii}(s_o)+(s-s_o)v(s_o)+ \qquad (2.88)$$

$$+\rho^2 \sum_{i=1}^{3} a_i\left[t_i(s_o)(1-\cos\frac{s-s_o}{\rho}) +\right.$$

$$\left. + n_i(s_o)(\frac{s-s_o}{\rho} - \sin\frac{s-s_o}{\rho})\right] = N_{ii}(s_o) + \rho^2\left[\underline{t}(s)-\underline{t}(s_o)\right]\cdot\nabla v$$

To return to our starting point $N_{11}(\tau)$ we need to know $s = s(\tau)$ given by

$$s = \int_{\tau_o}^{\tau} v(t)dt \qquad (2.89)$$

After some rearrangements we get from Ursin (1981A)

$$s(\tau) = s(\tau_o)+\rho 2\,\mathrm{arctg}\left\{\mathrm{tg}\left[\tfrac{1}{2}\theta(\tau_o)\right]\exp\left[\,|\nabla v|(\tau-\tau_o)\right]\right\} -$$

$$- \rho\theta(\tau_o) \qquad (2.90)$$

where

$$s(\tau_o) = s_o$$

and

$$\theta(\tau_o) = \arccos\frac{\underline{t}(\tau_o)\cdot\nabla v}{|\nabla v|} \qquad (2.91)$$

$\theta(\tau_o)$ is the angle between the tangent to the ray, $\underline{t}$, and the velocity gradient, ∇v, at $\tau = \tau_o$. In the case $\nabla v \parallel \underline{t}$ we get $v(s) = v(s_o)+|\nabla v|(s-s_o)\,\mathrm{sgn}(\nabla v\cdot\underline{t})$ and

$$N_{ii}(s) = N_{ii}(s_o)+v(s_o)(s-s_o)+\tfrac{1}{2}|\nabla v|(s-s_o)^2\,\mathrm{sgn}(\nabla v\cdot\underline{t}) \qquad (2.92)$$

We have now shown that in a medium with constant velocity gradient it is possible to find an explicit expression for the N_{ii} along the ray path. By equations (2.81) we have the expression for $K_{ii}(\tau)$, $R_{ii}(\tau)$ and $M_{ii}(\tau)$ as well. Hence the main problem in calculating the $J_i(\tau)$'s in equations (2.77) has now been reduced to the evaluation of the integral

$$\int_{\tau_o}^{\tau} v^2 M_{ii} d\tau \qquad i=1,2$$

Since both the expressions for v^2 and M_{ii} are rather complicated, we will not make any attempt to solve this integral analytically.

However, there is another way of calculating $J(\tau)$ which in our case turns out to be far simpler than the direct application of equations (2.77). Let us start with equation (2.66). Assuming constant velocity gradient and using (2.74) we get

$$\frac{dN}{d\tau} = v^2 I \tag{2.93}$$

Now let

$$\begin{aligned} T_N &= \mathrm{tr} N = N_{11}+N_{22} \\ D_N &= \det N = N_{11}N_{22}-N_{12}^2 \end{aligned} \tag{2.94}$$

From equation (2.93) we get

$$\frac{d}{d\tau} T_N = 2v^2 \tag{2.95}$$

$$\frac{d}{d\tau} D_N = v^2 T_N \tag{2.96}$$

Equations (2.43) and (2.68) give

$$\frac{1}{Jv}\frac{d}{d\tau}\left(\frac{J}{v}\right) = \frac{\partial}{\partial s}\left(\frac{1}{v}\right) + M_{11} + M_{22} = \frac{1}{v}\frac{d}{d\tau}\left(\frac{1}{v}\right) + M_{11} + M_{22} \tag{2.97}$$

Since $N = M^{-1}$ and therefore $T_M = T_N D_N^{-1}$, we write (2.97) as

$$\frac{dJ}{d\tau} = v^2 T_N D_N^{-1} J \tag{2.98}$$

Using equations (2.96) and (2.98) now finally gives

$$\frac{d}{d\tau}\left(\frac{J}{D_N}\right) = 0 \tag{2.99}$$

with solution

$$J(\tau) = \frac{J(\tau_o)}{D_N(\tau_o)} D_N(\tau) \tag{2.100}$$

where D_N is given by (2.94) and N_{ii} is given by (2.88), (2.90) and (2.91).

We observe that equation (2.100) is developed from equation (2.66) under one single constaint, namely, that of a constant velocity gradient.

The second version of equations (2.46) is in this special case written

$$U^{(o)}(\tau) = U^{(o)}(\tau_o) \left[\frac{N_{11}(\tau_o)N_{22}(\tau_o)v(\tau_o)\rho(\tau_o)}{N_{11}(\tau)N_{22}(\tau)v(\tau)\rho(\tau)}\right]^{\frac{1}{2}} \tag{2.101}$$

It is thus shown that the dynamic ray tracing in media with constant velocity gradient can be performed by use of analytical formulas to the lowest order in amplitude coefficients.

Analogous formulas to (2.101) using M instead of N are easily obtained by using (2.81).

2.11 The Riccati equation expressed in four equivalent systems of differential equations

As we have already concluded, the main problem in doing dynamic ray tracing is the solution of the Riccati equation. In this section we shall develop four equivalent systems of differential equations representing four different options for obtaining a numerical solution of the Riccati equation. Since equations (2.64) and (2.66) are the simplest expressions, we will concentrate our work on these. We will put the main effort in equation (2.66) and the results for equation (2.64) are seen to be quite similar. Equation (2.66) is given as

$$\frac{dN}{d\tau} - v^{-1}\, NVN = v^2 I$$

The elements of the matrix V are in this chapter written as $v_{ij} = v_{,ij}$. $i,j = 1,2$.

Let us assume initially that $N(\tau_o) = \begin{bmatrix} N_{11} & 0 \\ 0 & N_{22} \end{bmatrix}$ which is no loss of generality. We write

$$N = W\, U^{-1} \tag{2.102}$$

as suggested in Reid (1972), where

$$W = \begin{bmatrix} w_{11} & w_{12} \\ w_{21} & w_{22} \end{bmatrix}$$

$$U = \begin{bmatrix} u_{11} & u_{12} \\ u_{21} & u_{22} \end{bmatrix} \tag{2.103}$$

We claim U to be a solution of

$$\frac{dU}{d\tau} = VNU\,, \qquad U(\tau_o) = L \tag{2.104}$$

where L is nonsingular.

Equation (2.66) then transforms to

$$\frac{dW}{d\tau} = v^2 U$$

$$\frac{dU}{d\tau} = -v^{-1} VW \qquad (2.105)$$

Equations (2.105) represent 8 linear 1st order differential equations. Since we are free to choose the matrix L we set L = I. As initial conditions for equations (2.105) we therefore get, according to (2.102)

$$U(\tau_o) = I$$

$$W(\tau_o) = N(\tau_o) \qquad (2.106)$$

Let, as before, $D_U = \det U = u_{11}u_{22} - u_{12}u_{21}$. At each time, τ, along the ray the N_{ij} are given as

$$\begin{aligned} N_{11} &= D_U^{-1}[u_{22}w_{11} - w_{12}u_{21}] \\ N_{21} &= D_U^{-1}[u_{22}w_{21} - w_{22}u_{21}] \\ N_{12} &= D_U^{-1}[u_{11}w_{12} - w_{11}u_{12}] \\ N_{22} &= D_U^{-1}[u_{11}w_{22} - w_{21}u_{12}] \end{aligned} \qquad (2.107)$$

As we easily see from (2.107) this transformation has not utilized the general character of the matrix N, namely, that $N_{12} = N_{21}$. It is therefore natural to expect that the number of equations in (2.105) could be reduced without disturbing the linearity of the system. This reduction is obtained by introducing the following five new variables:

$$\begin{aligned} A &= D_W \\ B &= w_{11}u_{22} - w_{12}u_{21} \\ C &= w_{22}u_{11} - w_{21}u_{12} \\ D &= D_U \\ E &= w_{22}u_{21} - w_{21}u_{22} + w_{11}u_{12} - w_{12}u_{11} \end{aligned} \qquad (2.108)$$

The fact that $N_{12} = N_{21}$ leads to the equation

$$N_{21}D_U = u_{22}w_{21} - w_{22}u_{21} = u_{11}w_{12} - w_{11}u_{12} = N_{12}D_U \tag{2.109}$$

and therefore that

$$E = -2N_{21}D_U = -2N_{12}D_U \tag{2.110}$$

Equations (2.105) now yields the following 5 linear equations

$$\begin{aligned}
\frac{dA}{d\tau} &= v^2(C+B) \\
\frac{dB}{d\tau} &= v^2D - v^{-1}v_{22}A \\
\frac{dC}{d\tau} &= v^2D - v^{-1}v_{11}A \\
\frac{dD}{d\tau} &= -v^{-1}(v_{11}B + v_{22}C - v_{12}E) \\
\frac{dE}{d\tau} &= -2v^{-1}v_{12}A
\end{aligned} \tag{2.111}$$

with initial conditions

$$\begin{aligned}
A(\tau_o) &= N_{11}(\tau_o)N_{22}(\tau_o) \\
B(\tau_o) &= N_{11}(\tau_o) \\
C(\tau_o) &= N_{22}(\tau_o) \\
D(\tau_o) &= 1 \\
E(\tau_o) &= 0
\end{aligned} \tag{2.112}$$

At each time τ along the ray path the N_{ij} are given as

$$\begin{aligned} N_{11} &= B\ D^{-1} \\ N_{12} &= N_{21} = -\tfrac{1}{2}E\ D^{-1} \\ N_{22} &= C\ D^{-1} \end{aligned} \tag{2.113}$$

In this new system of functions it is also possible to find a simple expression for the Jacobian given in equation (2.69)

$$\begin{aligned} J(\tau) &= J(\tau_o)\exp\{\int_{\tau_o}^{\tau} v^2 \mathrm{tr}M\ d\tau\} \\ &= J(\tau_o)\exp\{\int_{\tau_o}^{\tau} v^2 D_N^{-1}\mathrm{tr}N\ d\tau\} \\ &= J(\tau_o)\exp\{\int_{\tau_o}^{\tau} (BC-(\tfrac{1}{2}E)^2)^{-1}D\ v^2(B+C)\ d\tau\} \\ &= J(\tau_o)\exp\{\int_{\tau_o}^{\tau} A^{-1}\frac{dA}{d\tau}\ d\tau\} \\ &= J(\tau_o)A(\tau_o)^{-1}A(\tau) \end{aligned} \tag{2.114}$$

That is, the Jacobian is seen to be proportional to $A(\tau)$ along the ray.

It is possible to reduce the number of equations even more ending up with a set of 4 <u>nonlinear</u> differential equations. The procedure is as follows:

We introduce a new function

$$G = AD - BC + (\tfrac{1}{2}E)^2 \tag{2.115}$$

Differentiating G with respect to τ gives

$$\frac{dG}{d\tau} = 0 \tag{2.116}$$

and thus G is invariant along the ray.

According to equations (2.112) we get $G(\tau_o) = 0$ and thus $G(\tau) = 0$ along the ray.

Letting

$$D = (BC - (\tfrac{1}{2}E)^2)A^{-1} \tag{2.117}$$

we get

$$\begin{aligned}
\frac{dA}{d\tau} &= v^2(C+B) \\
\frac{dB}{d\tau} &= v^2(BC - (\tfrac{1}{2}E)^2)A^{-1} - v^{-1}v_{22}A \\
\frac{dC}{d\tau} &= v^2(BC - (\tfrac{1}{2}E)^2)A^{-1} - v^{-1}v_{11}A \\
\frac{dE}{d\tau} &= -2v^{-1}v_{12}A
\end{aligned} \tag{2.118}$$

with initial conditions (2.112).

At each time τ along the ray the N_{ij} are given as

$$\begin{aligned}
N_{11} &= BA(BC-(\tfrac{1}{2}E)^2)^{-1} \\
N_{12} &= N_{21} = -\tfrac{1}{2}EA(BC-(\tfrac{1}{2}E)^2)^{-1} \\
N_{22} &= CA(BC-(\tfrac{1}{2}E)^2)^{-1}
\end{aligned} \tag{2.119}$$

and the Jacobian as in equation (2.114).

We observe that this new system is independent of D, but implicitly linked to D by equation (2.117). Equations (2.118) are singular at A=0. In the source point of the ray we have A=0.

Assuming A≠0 we introduce the new functions

$$b = B/A$$
$$c = C/A \qquad (2.120)$$
$$e = E/A$$

and get

$$\frac{db}{d\tau} = -v^2(b^2+(\tfrac{1}{2}e)^2)-v^{-1}v_{22}$$
$$\frac{dc}{d\tau} = -v^2(b^2+(\tfrac{1}{2}e)^2)-v^{-1}v_{11} \qquad (2.121)$$
$$\frac{de}{d\tau} = -v^2e(b+c)-2v^{-1}v_{12}$$

and

$$A(\tau) = A(\tau_o)\exp\{\int_{\tau_o}^{\tau} v^2(c+b)\,d\tau\}$$

giving

$$J(\tau) = J(\tau_o)\exp\{\int_{\tau_o}^{\tau} v^2(c+b)\,d\tau\} \qquad (2.122)$$

with initial conditions

$$b(\tau_o) = \frac{1}{N_{11}(\tau_o)} = M_{22}(\tau_o)$$
$$c(\tau_o) = \frac{1}{N_{11}(\tau_o)} = M_{11}(\tau_o) \qquad (2.123)$$
$$e(\tau_o) = 0$$

We easily see that (2.121) with (2.123) and (2.122) are the same equations as (2.64) and (2.69), respectively.

Introducing

$$A = (BC - (\tfrac{1}{2}E)^2)D^{-1} \tag{2.124}$$

instead of equation (2.117) and letting b = B/D, c = C/D and e = E/D would give equations (2.66).

If we had started the whole procedure with equation (2.64) instead of (2.66), we would instead of equations (2.105) have got

$$\begin{aligned} \frac{dW}{d\tau} &= -v^{-1}VU \\ \frac{dU}{d\tau} &= v^2W \end{aligned} \tag{2.125}$$

where $M = WU^{-1}$ and U is a solution of equation (2.104) with M instead of N. This result is obvious since $M = N^{-1}$. We observe that the treatment of equations (2.125) would be quite similar to the one we have just gone through with equations (2.105).

The question of which function, M or N, we want to use is dependent on which interval along the ray we want to integrate. For instance near the source the function M tends to inifinity and it would be more suitable to use the function N.

The question of which of the four equivalent sets of equations that should be used is determined by the numerical properties of the various sets of equations in the different regions of the medium. This problem will be treated in another section.

2.12 Crossing Curved Interfaces using Phase Matching

We shall now discuss the problem of ray tracing over discontinuities in the medium. A discontinuity will cause jumps both in the tangent vector (or slowness vector) and in the matrix M of second derivatives of the time field as well as in the amplitude coefficient.

To solve the discontinuity problem we shall use the phase matching method. We need an expansion of the phase function $\tau(s,q_1,q_2)$ at an arbitrary point $s = s_o$ on the ray. Let the point $(s_o,0,0)$ be denoted 0. To the second order we then get:

$$\tau(s,q_1,q_2) = \tau(s_o,0,0) + \frac{\partial\tau}{\partial s}\Big|_o (s-s_o) + \frac{1}{2}\frac{\partial^2\tau}{\partial s^2}\Big|_o (s-s_o)^2 + \frac{1}{2} q^T M q \qquad (2.126)$$

where the derivatives of τ and values of M are taken at 0 and q^T denotes a transposed matrix of $q = \begin{bmatrix} q_1 \\ q_2 \end{bmatrix}$.

According to (2.53) we get

$$\frac{\partial\tau}{\partial s}\Big|_o = \frac{1}{v(s_o)} \qquad \frac{\partial^2\tau}{\partial s^2}\Big|_o = -\frac{1}{v^2(s_o)}\, v_{,s} \qquad (2.127)$$

which gives

$$\tau(s,q_1,q_2) = \tau_o + v^{-1}(s-s_o) - \tfrac{1}{2} v^{-2} v_{,s}(s-s_o)^2 + \tfrac{1}{2} q^T M q \qquad (2.128)$$

where $\tau_o = \tau(s_o,0,0)$ and v, $v_{,s}$ and M are taken at 0.

We now transform equation (2.128) into a new auxiliary Cartesian coordinate system $[\ell,q_1,q_2]$ with the basis $\underline{t}$, $\underline{e}_1$, $\underline{e}_2$ at O. The new system has the same basis vectors at O as the ray centered coordinate system $[s,q_1,q_2]$. The only difference is that the system $[\ell,q_1,q_2]$ is Cartesian, whereas the ray centered coordinate system $[s,q_1,q_2]$ is curvilinear.

For fixed q_1 and q_2 the element $d\ell$ in the Cartesian system is related to the element ds by the formula $d\ell = h\,ds$ where h is defined in equation (2.55). Thus for small $s-s_o$ we write

$$s-s_o = h^{-1}\ell = \ell - v^{-1}(q_1 v_{,1}+q_2 v_{,2})\ell \qquad (2.129)$$

Inserting this into (2.128) we get, to the second order

$$\tau(\ell,q_1,q_2) = \tau_o + v^{-1}\ell - v^{-2}(q_1 v_{,1}+q_2 v_{,2})\ell - \tfrac{1}{2}\, v^{-2} v_{,s}\ell^2 + \tfrac{1}{2}\, q^T M q \qquad (2.130)$$

All quantities $\tau_o, v, v_{,1}, v_{,2}, v_{,s}$ and M are taken at O.

Now let O be the point where the ray strikes the curved interface, S. The phase matching method requires that the phase function of incident, reflected and transmitted waves be equal on S in the vicinity of O.

We now construct a local Cartesian coordinate system $[n,d_1,d_2]$ at O with basis $\underline{n}$, $\underline{d}_1$, $\underline{d}_2$ such that:

$\underline{n}$ is a normal vector to the curved interface at O, pointing into the medium containing the incident wave; (should not be confused with the $\underline{n}$ introduced in section 2.4 which was the normal vector to the ray)

$\underline{d}_1$ is oriented along the intersection of the plane of incidence with the tangent plane to the interface at O in such a way that it makes an acute angle with the unit tangent $\underline{t}$ to the ray of incident wave at O;

$\underline{d}_2$ is a tangent vector to the interface at O being defined as a cross-product $\underline{d}_2 = \underline{n} \times \underline{d}_1$. (Note that $\underline{d}_2$ is perpendicular to the plane of incidence.)

Let it now be assumed that the basis vector $\underline{e}_2$ in the auxiliary Cartesian coordinate system pertinent to the incident ray coincides with the basis vector $\underline{d}_2$. (If this is not the case, a simple rotation of the auxiliary system at O about the vector $\underline{t}$ would do.)

The Cartesian coordinate system $[\ell, q_1, q_2]$ is linked to the local coordinate system $[n, d_1, d_2]$ through the transform

$$\begin{aligned} q_1 &= \pm\, d_1 \cos \iota - n \sin \iota \\ q_2 &= d_2 \\ \ell &= d_1 \sin \iota \pm n \cos \iota \end{aligned} \tag{2.131}$$

where ι is an acute angle between the tangent to the ray at O and $\underline{n}$. The upper sign in (2.131) corresponds to the reflected rays whereas the lower sign is to be taken for the incident and transmitted rays. Inserting (2.131) into (2.130), we obtain a new expression for the phase function $\tau(n, d_1, d_2)$ in the coordinates $[n, d_1, d_2]$ in the vicinity of O, with accuracy up to the second order in n, d_1 and d_2. We now seek the value of τ along the interface and denote it τ_I. We describe the interface by $n = n(d_1, d_2)$. In the neighborhood of O, with accuracy up to the second order in d_1 and d_2, this reduces to

$$n = -\tfrac{1}{2}\, d^T D d \tag{2.132}$$

where d^T is the transposed matrix of $d = \begin{bmatrix} d_1 \\ d_2 \end{bmatrix}$ and D is the curvature matrix of the interface S at O. The minus sign indicates that the positive curvatures were chosen for those parts of the interface that are seen as convex by an observer located in the medium containing incident wave. It follows from (2.131) and (2.132) that

$$q = Hd + O(d^2), \qquad H = \begin{bmatrix} \pm \cos \iota & 0 \\ 0 & 1 \end{bmatrix} \tag{2.133}$$

Let $\tau_I(d_1,d_2) = \tau[n(d_1,d_2), d_1,d_2]$. Inserting (2.131), (2.132) and (2.133) into (2.130) we get

$$\begin{aligned}\tau_I(d_1,d_2) = \tau_o &+ v^{-1}\sin\iota\, d_1 \mp \tfrac{1}{2}v^{-1}\cos\iota\, d^T D d \\ &- v^{-2}(\pm\, d_1 \cos\iota\, v_{,1} + d_2 v_{,2}) d_1 \sin\iota \\ &- \tfrac{1}{2}\, v^{-2}\, v_{,s} d_1^2 \sin^2\iota + \tfrac{1}{2}\, d^T H M H d\end{aligned} \tag{2.134}$$

in the vicinity of O with accuracy up to the second order in d_1 and d_2.

Written more compactly in matrix form we have

$$\tau_I(d_1,d_2) = \tau_o + v^{-1}\sin\iota\, d_1 + \tfrac{1}{2}\, d^T F d \tag{2.135}$$

where

$$F = HMH \mp v^{-1}\cos\iota\, D - v^{-2}\sin\iota \begin{bmatrix} \pm 2v_{,1}\cos\iota & v_{,2} \\ v_{,2} & 0 \end{bmatrix} - \frac{\sin^2\iota}{v^2}\begin{bmatrix} v_{,s} & 0 \\ 0 & 0 \end{bmatrix} \tag{2.136}$$

The upper signs in (2.134) and (2.136) correspond to reflected waves, while the lower signs are related to the incident and transmitted waves. All values of v, $v_{,1}$, $v_{,2}$, $v_{,s}$ and M are taken at O.

We are now ready to do the phase matching. Let the tilde above the symbols denote the quanitities pertinent to the reflected and transmitted waves to distinguish them from the incident waves. The phase matching is then expressed as $\tau_I = \tilde{\tau}_I$ for all d near O. This results in two equations. The first is recognised as Snell's law

$$v^{-1} \sin\iota = \tilde{v}^{-1} \sin\tilde{\iota} \tag{2.137}$$

and the second equation is

$$F = \tilde{F} \tag{2.138}$$

Using equation (2.136) we get for (2.138):

$$\tilde{M} = SMS + uGDG + \frac{\sin \iota}{v} GEG \tag{2.139}$$

where

$$S = \begin{bmatrix} \pm \frac{\cos \iota}{\cos \tilde{\iota}} & 0 \\ 0 & 1 \end{bmatrix}, \quad G = \begin{bmatrix} \pm \frac{1}{\cos \tilde{\iota}} & 0 \\ 0 & 1 \end{bmatrix},$$

$$E = \begin{bmatrix} E_{11} & E_{12} \\ E_{12} & 0 \end{bmatrix}, \quad u = \left(\frac{\cos \iota}{v} \pm \frac{\cos \tilde{\iota}}{\tilde{v}} \right),$$

$$E_{11} = 2\left(\frac{v,1}{v} \cos \iota \pm \frac{\tilde{v},1}{\tilde{v}} \cos \tilde{\iota}\right) - \frac{\sin \iota}{v} (v,s - \tilde{v},s) \quad \text{and}$$

$$E_{12} = -\frac{v,2}{v} + \frac{\tilde{v},2}{\tilde{v}}$$

are evaluated at the point of incidence O. In this manner all matrices $\tilde{M}$ for the reflected and transmitted waves are fully determined at O, provided that the velocity structure in both layers is known in the vicinity of the point of incidence together with the geometrical shape of the interface. We observe that the matrix D vanishes if we have a plane interface and that the matrix E vanishes in the case of homogeneous layers.

2.13 Changes in Amplitude Crossing Curved Interfaces

Up to this point we have only discussed discontinuities in the matrix M and in the direction of the ray. We will now make some comments on the change in amplitude coefficient. We shall call an interface at which the n-th derivative of the elastic parameters or density are discontinuous, an interface of (n+1)-th order; at the interface of first order the elastic parameters or density themselves are discontinuous. According to Cerveny et al (1977) we generally have that in the case of the interface of (n+1)-th order, the reflected and transmitted waves are of n-th order. All interfaces treated in this thesis will be of first order and thus the reflected and converted transmitted waves are of the zero-th order. From Cerveny et al (1977) we then have:

i) When a P or SV wave impinges on an interface of the first order, only P and SV reflected and transmitted waves are generated.
ii) When an SH wave impinges on an interface of the first order, only SH reflected and transmitted waves are generated.
iii) The ratio of any principal component of a reflected (transmitted) wave to any principal component of the incident wave at the point O does not depend on the curvature of the interface, on the curvature of the wave front of the incident wave, or on any derivative of the elastic parameters. Obviously, it does not depend on the shape of the incident pulse, either. It depends only on the angle of incidence and on the elastic parameters and density at O (on both sides of the interface).

Here SH is the component of the S-wave parallel to the interface and SV is the component perpendicular to this direction.

It follows from iii) that the ratios of the principal components in our case are given by standard reflection and transmission coefficients of plane waves at a plane interface between two homogeneous media.

We also conclude that the reflection and transmission coefficients are of two types: P-SV coefficients and SH coefficients. These so-called displacement coefficients are presented in Cerveny et al (1977).

We shall list the reflection/transmission coefficients for P waves only since these are referred to in a later chapter.

Let α_1,β_1 be P and S velocities, respectively, at one side of an interface and let α_2,β_2 be the corresponding velocities at the other side of the interface. Let further

$$\begin{aligned} P_1 &= [1 - (\alpha_1 p)^2]^{\frac{1}{2}} \\ P_2 &= [1 - (\beta_1 p)^2]^{\frac{1}{2}} \\ P_3 &= [1 - (\alpha_2 p)^2]^{\frac{1}{2}} \\ P_4 &= [1 - (\beta_2 p)^2]^{\frac{1}{2}} \end{aligned} \qquad (2.140)$$

where

$$p = \frac{|\underline{n} \times \underline{t}|}{\alpha_1}$$

$\underline{n}$ is defined in section 2.12 and $\underline{t}$ is as before the tangent vector to the ray at the incident side of the interface. According to Snell's law p is constant when crossing the interface.

If ρ_i, i=1,2, are the densities of the two interfacing media we define

$$\begin{aligned} q &= 2(\rho_2\beta_2^2 - \rho_1\beta_1^2) \\ X &= \rho_2 - qp^2 \\ Y &= \rho_1 + qp^2 \\ Z &= \rho_2 - \rho_1 - qp^2 \end{aligned} \qquad (2.141)$$

and

$$\begin{aligned} D = {} & q^2p^2P_1P_2P_3P_4 + \rho_1\rho_2(\beta_1\alpha_2P_1P_4 + \alpha_1\beta_2P_2P_3) + \\ & \alpha_1\beta_1P_3P_4Y^2 + \alpha_2\beta_2P_1P_2X^2 + \alpha_1\alpha_2\beta_1\beta_2p^2Z^2 \end{aligned} \qquad (2.142)$$

The reflection coefficient for P waves is then given as

$$R_p = D^{-1}[q^2p^2P_1P_2P_3P_4 + \rho_1\rho_2(\beta_1\alpha_2P_1P_4 - \alpha_1\beta_2P_2P_3) - \\ - \alpha_1\beta_1P_3P_4Y^2 + \alpha_2\beta_2P_1P_2X^2 - \alpha_1\alpha_2\beta_1\beta_2p^2Z^2] \tag{2.143}$$

and the transmission coefficient is given as

$$T_p = 2\alpha_1\rho_1P_1(\beta_2P_2X + \beta_1P_4Y)D^{-1} \tag{2.144}$$

It is a well known fact that the P velocity (α_i) is greater than the S velocity (β_i). We thus have that the P_is in (2.140) are real numbers except in the case where the angle of incidence is greater than the angle of critical refraction for P waves. P_i represents the sine of the angle of reflection/transmision for the different ray types (reflected P, reflected SV, transmitted P, transmitted SV), and therefore P_3 (and for great angles of incidence also P_4) is set to zero when $(p\alpha_2)^2$ (or $(p\beta_2)^2$) is greater than one.

2.14 Source Functions

For the completeness of the theory we include some comments on the choice of source functions. The problem is how to represent the function $\phi^{(o)}(\gamma_1,\gamma_2)$ in equation (2.46) or in other words the initial conditions of the dynamic ray tracing system at the source. We shall consider only the simplest types of source functions, that is, the point source and the linear source. For more complicated source functions we refer to Aki and Richards (1980).

We assume the medium in some small neighborhood of the source to be homogeneous. In most applications this is no strong restriction. Let v_o and ρ_o denote the values of v and ρ in this neighborhood. Replace the ray parameters in equation (2.46), γ_1,γ_2, with the take-off angles, δ_o and θ_o, in the case of a point source and with δ_o and ℓ_o in the case of a linear source. Here θ_o is the azimuth, δ_o is the angle of the ray with the horizontal (or any other reference) plane and ℓ_o is the position coordinate along the linear source.

In the homogeneous medium we may compute the exact solutions of the equations of motion and the expressions for the Jacobian function, J, for a point and linear source. Comparing the exact solutions with equation (2.46) gives us the following fomulas for $\phi^{(o)}$:

i) Point source $$\phi^{(o)} = (v_o\rho_o \sin\delta_o)^{\frac{1}{2}} g^*(\delta_o,\theta_o) \tag{2.145}$$

ii) Linear source $$\phi^{(o)} = (v_o\rho_o)^{\frac{1}{2}} g^{**}(\delta_o) \tag{2.146}$$

The functions g* and g** are directional characteristics of the ray and describe the distribution of the amplitude coefficient, $U_o^{(o)}$, on a unit sphere or a unit circle, respectively, with their centers at the source. If no directions are preferred, then g* and g** are constant functions of their parameters.

For the amplitude coefficient we get

i) Point source $$U_o^{(o)}(\tau) = \left(\frac{\sin\delta_o}{J(\tau)}\right)^{\frac{1}{2}} g^*(\delta_o,\theta_o)\left(\frac{v_o\rho_o}{v(\tau)\rho(\tau)}\right)^{\frac{1}{2}} \tag{2.147}$$

ii) Linear source $$U_o^{(o)}(\tau) = (J(\tau))^{-\frac{1}{2}} g^{**}(\delta_o)\left(\frac{v_o\rho_o}{v(\tau)\rho(\tau)}\right)^{\frac{1}{2}} \tag{2.148}$$

This is valid for both the S wave components as well as for the P wave due to the decoupling of the S components in the $\underline{e}_1,\underline{e}_2,\underline{t}$ basis.

3. NUMERICAL IMPLEMENTATION OF THEORY

In this chapter we shall present the numerical algorithms needed to perform dynamic ray-tracing in a general 3-D model.

First of all we must find a way to represent our model. We have divided this part into three sections:

i) representing the interfaces
ii) representing the velocities
iii) representing the densities.

In this thesis the interfaces are defined as surfaces along which the velocity or the density is discontinuous. We permit the interfaces to have any curvatures, but we claim that they are twice differentiable almost everywhere. This is sufficient if we want to use the phase-matching principle described in chapter 2.12. The application of equation (2.132) assumes that the interface is smooth in the vicinity of the intersection point between the ray and the interface. In section 3.1 we describe the different kinds of interfaces to be used and we find the relations between equation (2.132) and the interfaces specified.

The representation of the velocities in the layers between the interfaces is a very important part of this chapter. It is a well known fact that the amplitude coefficient is very sensitive to the velocity. This has been demonstrated in a 2-D model by Cerveny et al (1977). We claim that the velocity function must be twice differentiable everywhere between the interfaces. Dynamic ray-tracing through points where the velocity is discontinuous in some of the derivatives up to the second order does not make any sense since for instance formula (2.58) assumes the existence of these derivatives. The velocity functions used in this thesis are divided into two groups:

i) second order polynomials in x,y and z
ii) spline functions.

The density representation is of no importance as far as the ray path is concerned, but it is significant in the evaluation of amplitude coefficients both at the interfaces (see section 2.13) and in the media between the interfaces (equations (2.46)). Between the interfaces we must represent the density as a continuous function of space coordinates.

After the model has been specified, our problem will be how to trace a ray through the different layers. Thus, given a source position, an initial direction for the ray and a pointer to the interfaces which should act as reflectors to the ray, find a procedure to trace the rays effectively through the model.

It is important to use the analytic solutions when they can be found, and to have an efficient procedure for integrating the differential equations in the general case. In section 3.4 we find algorithms for tracing a ray a given distance s in a given model. The problem of how to trace through interfaces is properly handled by sections 2.12, 2.13 and 3.5.

The last section in this chapter is a description of a search process to determine the intersection point between the ray and the interface. In some special cases this intersection point may be found analytically, but in general a search procedure is needed.

3.1 Representing the Interfaces

In this and the following sections we shall treat the problem of how to represent a 3-D model. Before turning to the detailed procedure, we shall state the following requirements:

i) The model representation should be general enough to include models of relatively high complexity (faults, discontinuities, continuously variating velocity gradients, smooth surfaces of any curvatures, etc.).

ii) Enough information should be specified to assure that a ray starting from an arbitrary point in the model can be effectively traced through the model, being reflected/refracted at the proper interfaces.

iii) The manual effort in specifying the model parameters should be kept within reasonable limits.

Obviously, the more details we put into the model, the more manual effort is needed in specifying it and the less efficient is the tracing. To describe the model, we define the space of definition of the model as

$$S_d = \{(x,y,z) | (x,y) \in [a,b] \times [c,d]\} \tag{3.1}$$

where (x,y) are the horizontal coordinates and z is the depth coordinate. We call the rectangle $[a,b] \times [c,d]$ the rectangle of definition or just R_d.

All points (x,y,z) with horizontal coordinates not inside the rectangle of definition are defined to be outside the model. The depth boundaries are defined by the interfaces.

To perform the dynamic ray-tracing we must claim that the interfaces are continuous and have continuous 1st and 2nd derivatives almost everywhere on R_d. Generally this condition is satisfied if we represent the interfaces by spline functions (Ahlberg et al, 1967; Gjøystdal, 1979).

We will use the following three functions as interfaces in our procedure:

i) dipping plane
ii) cylindrical cubic spline surface
iii) general bicubic spline surface.

The cylindrical cubic spline surface is represented by a depth function

$$z = z(x,y) = z(x), \quad (x,y) \in [a,b] \times [c,d].$$

The function is specified by a set of sample points in the xz-plane, through which a cubic spline curve is fitted. The sample points are given at constant intervals along the x-axis (see Fig. 3.1),

$$(x_i,z_i), \qquad x_i = x_1 + (i-1)\Delta x , \qquad i = 1,n \tag{3.2}$$

where

x_1 is the first sample point

Δx is the constant sampling interval

i is the sample index

n is the number of samples

z_i is the functional value at x_i.

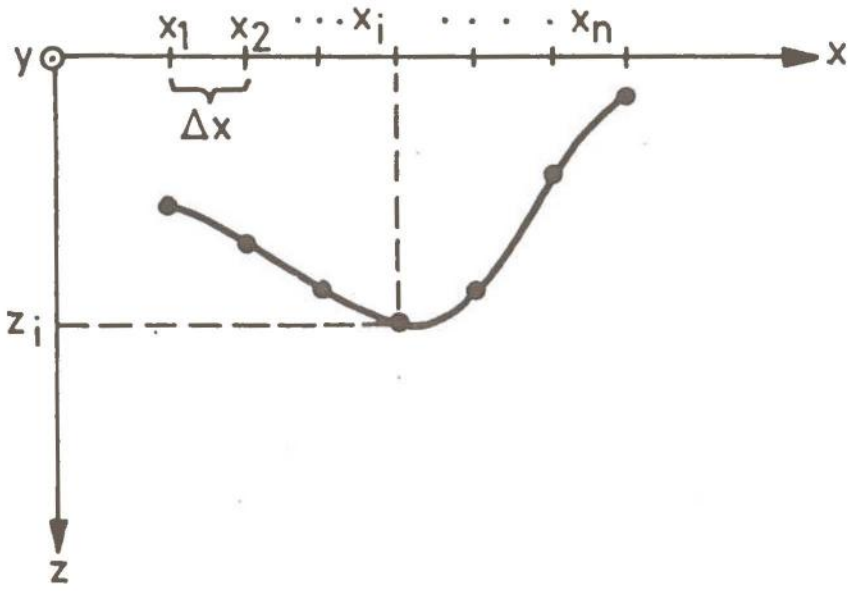

Fig. 3.1 Cylindrical cubic spline function. y-axis out of paper plane.

On each of the n-1 intervals the function is defined by 4 spline coefficients

$$c_{i1},\ c_{i2},\ c_{i3},\ c_{i4}\ , \qquad i = 1,\ n-1 \tag{3.3}$$

For the i-th interval $x_i \leq x \leq x_{i+1}$ we have

$$z(x) = \sum_{k=1}^{4} c_{ik}(x-x_i)^{k-1} \tag{3.4}$$

Thus we see that c_{i1} is the functional value in x_i, that is, $c_{i1} = z_i$.

To summarize, each simple interface can in this case be described by a sequence of 4(n-1)+3 parameters:

$$x_1, \Delta x, n, (c_{ik},\ k=1,4,\ \ i=1,n-1) \tag{3.5}$$

The general bicubic spline surface is specified by the z-values on a uniform rectangular grid in the xy-plane (see Fig. 3.2).

$$z = z(x,y)\ ,\quad (x,y) \in [a,b] \times [c,d]$$

Sample points (x_i, y_j, z_{ij}) are given as follows:

$$\begin{aligned} x_i &= x_1 + (i-1)\ \Delta x \qquad & i &= 1,n \\ y_j &= y_1 + (j-1)\ \Delta y \qquad & j &= 1,m \end{aligned} \tag{3.6}$$

z_{ij} - depth value in grid point (x_i, y_j).

A bicubic spline surface is fitted through the data points, and 16 coefficients are determined on each of the (n-1) • (m-1) rectangles:

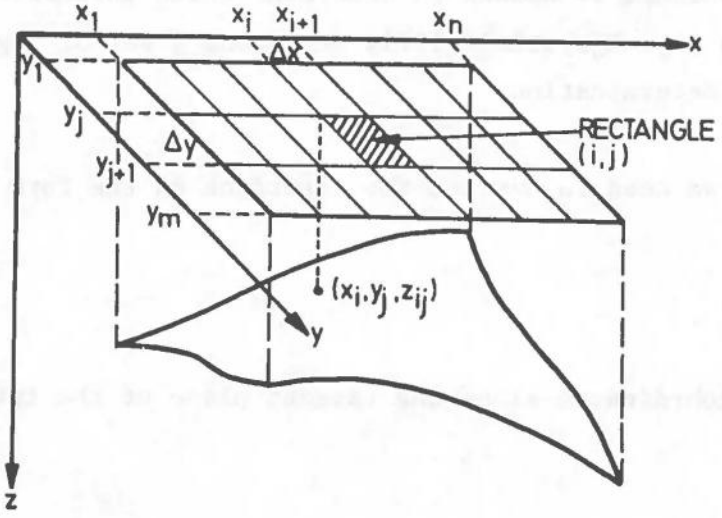

Fig. 3.2 General bicubic spline surface.

For a point (x,y) located within the ij-th rectangle, that is, $x_i \leq x \leq x_{i+1}$ and $y_j \leq y \leq y_{j+1}$, we have

$$z(x,y) = \sum_{k=1}^{4} \sum_{\ell=1}^{4} c_{ijk\ell}(x-x_i)^{k-1}(y-y_j)^{\ell-1} \tag{3.7}$$

Note that c_{ij11} is the depth value in (x_i,y_j), that is, $c_{ij11} = z_{ij}$.

To summarize, each simple interface may be described by a sequence of $16(n-1)(m-1)+6$ parameters:

$$c_1,\Delta x,n,y_1,\Delta y,m,(c_{ijk\ell},\ k=1,4,\ \ \ell=1,4,\ \ i=1,n-1,\ \ j=1,m-1) \tag{3.8}$$

Note that the rectangle of definition of the interface function, $[a,b] \times [c,d]$, need not be equal to the rectangle $[x_1,x_n] \times [y_1,y_n]$. The latter rectangle may be contained within the former, or the opposite may be true. This means that one has the possibility of sampling the function outside the area of definition, and that one also may extrapolate the functional values outside the given grid. In the latter case the coefficients of the closest rectangle are used in the computation of the functional value. Note also that in the 2-D case we may use cylindrical spline surfaces.

In the more complex cases like faults and intersections of interfaces, a more sophisticated procedure is needed to determine which interface to be considered for a given ray. Gjøystdal (1979) describes a set of logical tests to perform this determination.

As mentioned earlier, we need to express the interface on the form

$$n = -\tfrac{1}{2}\, d^T D d \tag{3.9}$$

where $d = \begin{bmatrix} d_1 \\ d_2 \end{bmatrix}$ are coordinates along the tangent plane of the interface,

D is the curvature matrix and n is the coordinate normal to the interface. The origin of this system is at the point of reflection/refraction. What we need is a relation between the matrix D and the 2nd derivatives of the interface at the point of refraction/reflection. Let (x_o,y_o,z_o) be this point in the $[x,y,z]$ coordinate system. The interface may then be approximated by a second order surface

$$z = f(x,y) = a_{11}(x-x_o)^2+a_{12}(x-x_o)(y-y_o)+a_{22}(y-y_o)^2+$$

$$b_1(x-x_o)+b_2(y-y_o)+z_o \qquad (3.10)$$

where the constants a_{ij} and b_i have values such that all first and second order derivatives of the function f are equal to the derivatives of the interface at the point (x_o,y_o,z_o). Let us further, for reasons of simplicity, assume that the point (x_o,y_o,z_o) is the origin of the x,y,z-system. This is no loss of generality. The problem is now reduced to finding the relations between the elements of the matrix D and the constants a_{ij},b_i in the function

$$z = f(x,y) = a_{11}x^2+a_{12}xy+a_{22}y^2+b_1x+b_2y \qquad (3.11)$$

We define the matrices A,B and X as

$$A = \begin{bmatrix} a_{11} & a_{12} & 0 \\ a_{12} & a_{22} & 0 \\ 0 & 0 & 0 \end{bmatrix}$$

$$B = [\ b_1,b_2,-1\ ]^T \qquad (3.12)$$

$$X = [\ x,y,z\ ]^T$$

and write relation (3.11) as

$$X^TAX + B^TX = 0 \qquad (3.13)$$

where T as before denotes transposition.

Let Q be defined as a rotational matrix between the x,y,z-system and the n,d_1,d_2-system such that

$$X = QX' \tag{3.14}$$

where

$$X' = [d_1, d_2, n]^T$$

For equation (3.13) we then get

$$X'^T Q^T A Q X' + B^T Q X' = 0 \tag{3.15}$$

We define

$$\left.\begin{aligned} P &= \begin{bmatrix} P11 & P12 & P13 \\ P21 & P22 & P23 \\ P31 & P32 & P33 \end{bmatrix} = Q^T A Q \\ \text{and} \\ C &= [c_1, c_2, c_3]^T = Q^T B \end{aligned}\right\} \tag{3.16}$$

to get

$$X'^T P X' + C^T X' = 0 \tag{3.17}$$

By evaluating the first and second derivatives of equation (3.17) at the origin, we get the relations:

$$\frac{\partial^2 n}{\partial d_1^2} = -\frac{2p_{11}}{c_3}$$

$$\frac{\partial^2 n}{\partial d_2^2} = -\frac{2p_{22}}{c_3} \qquad (3.18)$$

$$\frac{\partial^2 n}{\partial d_1 \partial d_2} = -\frac{2p_{12}}{c_3}$$

Comparing these with the values of the function (3.9) gives us

$$d_{11} = +\frac{2p_{11}}{c_3}$$

$$d_{12} = +\frac{2p_{12}}{c_3} \qquad (3.19)$$

$$d_{22} = +\frac{2p_{22}}{c_3}$$

We have thus found the relations between the derivatives of the given interface and the matrix $D = \begin{bmatrix} d_{11} & d_{12} \\ d_{12} & d_{22} \end{bmatrix}$. The p_{ij} and c_3 are well defined from equations (3.16) as soon as we know the rotational matrix Q.

3.2 Representing the velocities

In performing the dynamic ray tracing in the general case we need to calculate the values of the following functions along the ray:

$$v, \quad \nabla v, \quad \frac{\partial v}{\partial q_i}, \quad \frac{\partial^2 v}{\partial q_i \partial q_j}, \qquad i,j = 1,2 \qquad (3.20)$$

It can be shown (Cerveny et al, 1977) that the ray method is very sensitive to the representation of the velocity function. Especially piece-wise linear interpolation of velocity between mesh points will not do. This causes enormous (and unrealistic) fluctuations in amplitude coefficients over an array, even though the obtained travel times seem correct. These fluctuations are due to the fact that linear interpolation causes false interfaces of the second order to appear which exert great effect on the amplitude. It is thus important that the velocity function is smooth. In addition we claim that the representation of the velocity is such that the values (3.20) can be estimated at any point of any ray in the model. That is, we want the velocity to be an analytic function of space coordinates.

We propose two ways of representing the velocity. The first representation is a very simple polynomial in x,y, and z. In the case of constant velocity gradient we have

$$v(x,y,z) = a_o+a_1x+a_2y+a_3z \tag{3.21}$$

and up to the second order, we get

$$v(x,y,z) = a_o+a_1x+a_2y+a_3z+b_{11}x^2+b_{12}xy+b_{13}xz+b_{22}y^2+b_{23}yz+b_{33}z^2 \tag{3.22}$$

The case of constant velocity gradient is particularly important since we found analytical solutions of the differential equations for such velocity structures in section 2.10.

The second approach is more practical and includes the use of splines (Ahlberg et al, 1967). Let us assume that we know the velocity at both sides of two interfaces. The problem is how to model the velocity in the medium separated by the interfaces. This is a quite common situation in applications. Let interface 1 be described by a bicubic spline function $z_1(x,y)$ and let $v_1(x,y)$ be a bicubic spline function representing the velocity at the side of interface 1 directed towards interface 2. Further on, let $z_2(x,y)$ be a spline describing interface 2 and $v_2(x,y)$ be a spline representing the velocity

at the side of interface 2 directed towards interface 1. We may then describe the velocity in the medium by

$$v(x,y,z) = v_1(x,y) + \frac{v_2(x,y)-v_1(x,y)}{z_2(x,y)-z_1(x,y)} (z-z_1(x,y)) \qquad (3.23)$$

This is a smooth function having well defined derivatives and second derivatives in any direction provided that the splines z_1 and z_2 do not intersect. The function has a kind of 'preferred' direction along the z-axis since the velocity variation along this direction is linear. If we had even more knowledge of the medium, we could modify equation (3.23) slightly. Let us assume for instance that we wanted the medium to have a certain velocity $v_3(x,y)$ at a surface $z_3(x,y)$ lying in between z_1 and z_2 and without disturbing the smoothness of the velocity function between z_1 and z_2. We could then write

$$v(x,y,z) = v_1(x,y) + \frac{v_2(x,y)-v_1(x,y)}{z_2(x,y)-z_1(x,y)} (h(x,y,z)-z_1(x,y)) \qquad (3.24)$$

where $h(x,y,z)$ is a spline function along the z-axis such that

$$\begin{aligned} h(x,y,z_1) &= z_1(x,y) \\ h(x,y,z_2) &= z_2(x,y) \\ h(x,y,z_3) &= z_1(x,y)+(v_3(x,y)-v_1(x,y)) \frac{z_2(x,y)-z_1(x,y)}{v_2(x,y)-v_1(x,y)} \end{aligned} \qquad (3.25)$$

This approach could easily be extended to take into account any number of surfaces of known velocities between the two interfaces.

The choice of the 'preferred' direction (z-axis) is dependent on the application of the method. One important task is to avoid 'unnatural' osciallations in the velocity function along the ray. Such oscillations can be problematic using spline functions. In oil exploration seismic reflection studies most experiments use rays which are close to vertical and therefore it would be best to use a

velocity function with a simple variation in z to avoid serious oscillations. In addition to the preferred direction we do also have the derivatives at the endpoints of the 1-D spline, $h(x_o,y_o,z)$, at our disposal for controlling the oscillations.

From these velocity models ∇v and $\partial^2 v/\partial x_i \partial x_j$ can be computed analytically and likewise $\partial v/\partial q_i = \underline{e}_i \cdot \nabla v$, where $\underline{e}_i$ is defined in equations (2.21). Letting $\underline{e}_i$ be decomposed as $\underline{e}_i = (e_{ix_1}, e_{ix_2}, e_{ix_3})$, we get for the double derivatives

$$\frac{\partial^2 v}{\partial q_i \partial q_j} = \sum_{\substack{k=1 \\ \ell=1}}^{3} e_{ix_k} e_{jx_\ell} \frac{\partial^2 v}{\partial x_k \partial x_\ell} \tag{3.26}$$

Letting $z_1(x,y)$ and $z_2(x,y)$ be planes z = const. and $v_1(x,y) = v_2(x,y)$, give us a two-dimensional velocity model

$$v(x,y) = v_1(x,y) \tag{3.27}$$

where $v_1(x,y)$ is again the bicubic spline. Tracing in a plane z = const. leads to a pure 2-D consideration.

Since the ray always turns towards the direction of the gradient of 1/v (Hudson, 1980), we could in some critical numerical cases overcome the difficulties by representing (1/v) instead of v.

3.3 Representing the densities

As we stated in the introductory remarks to this chapter, the density must be a continuous function of space between the interfaces. However, to the lowest order in amplitude coefficient (see equations (2.46)) we do not need to know the density anywhere except at both sides of the interfaces. For higher order evaluations we need to integrate the density along the ray (equations (2.45)) and thus the density variations are of greater importance

in these cases. We have chosen to represent the density in the same way as we did with the velocity. Thus, by changing v with ρ, the density representation could be described by equations (3.22), (3.24) or special cases of these.

3.4 Dynamic Ray Tracing in a Continuous Medium

As we have already stated in Section 2 the ray tracing system is described by a set of six ordinary differential equations

$$\frac{dx_i}{d\tau} = v^2 p_i \,, \quad \frac{dp_i}{d\tau} = -v^{-1} \frac{\partial v}{\partial x_i} \,, \qquad i = 1,2,3 \tag{3.28}$$

where x_i are the coordinates of the ray at time τ, $p_i = \partial\tau/\partial x_i$ are the components of the slowness vector and v is the velocity of the wave ($v = \alpha$ for P waves and $v = \beta$ for S waves).

An equivalent system to (3.28) expressed in terms of tangent vector to the ray instead of slowness vector would be

$$\frac{dx_i}{d\tau} = v t_i \,, \quad \frac{dt_i}{d\tau} = \frac{dv}{ds} t_i - \frac{\partial v}{\partial x_i} \,, \qquad i = 1,2,3 \tag{3.29}$$

where $t_i = v p_i$ are the components of the tangent vector. (See for instance Shah (1973) for details.)

Together with one of these sets we have to solve one of the equations (2.64), (2.65), (2.66) or (2.67). We have chosen

$$\frac{dM}{d\tau} + v^2 M^2 = -v^{-1} V \tag{3.30}$$

and

$$\frac{dN}{d\tau} - v^{-1} N V N = v^2 I \tag{3.31}$$

because of their simple form.

Equation (3.30) has the disadvantage that M tends to infinity near the source and for instance at focus points, while N in (3.31) tends to infinity when the wave approaches a plane wave.

Other equivalent sets like equations (2.105), (2.111) and (2.118) will also be considered.

As we have already shown, these sets have analytical solutions for some simple velocity models. In the case of constant velocity, the rays are straight and the tracing is easy to perform. If $\nabla v \neq \underline{0}$, but constant, the tracing is a bit more complicated. We have two possibilities:

i) $\nabla v \parallel \underline{t}$

ii) $\nabla v \not\parallel \underline{t}$

where $\underline{t}$ is the tangent vector of the ray. In the first case the rays are straight and in the second case they are circular according to equation (2.84). The wavefront curvatures are in the first case found by using equation (2.92), while we in the second case apply (2.88). For more complex velocity structures we will have to find numerical solutions of the differential equations.

We have considered both the Runge-Kutta method and the Adams method. The first-mentioned is the simplest and in several respects the best understood, but it is the least efficient. We have chosen to use a modified divided difference form of the Adams PECE (Predict-Evaluate-Correct-Evaluate) formulas and local extrapolation. This approach has shown to be very suitable for our use and is far more efficient than the Runge-Kutta methods. To describe the algorithm briefly, we introduce the intial-value problem

$$\begin{aligned} y'(x) &= f(x,y(x)) \\ y(a) &= A \\ x &\in [a,b] \end{aligned} \qquad (3.32)$$

where y, A and f in general may be vectors.

We want to approximate the solution on a mesh, generally separated by unequal step sizes $h_1, h_2, h_3, \ldots$ so that

$$x_o = a$$
$$x_n = x_{n-1} + h_n \qquad n = 1,2,\ldots \tag{3.33}$$

Let y_n be an approximation to the solution $y(x)$ of equations (3.32) at the mesh point x_n:

$$y_n \approx y(x_n) \tag{3.34}$$

Because $y(x)$ satisfies (3.32), an approximation of $y(x_n)$ leads to an approximation of $y'(x_n)$, namely:

$$f_n = f(x_n,y_n) \approx y'(x_n) = f(x_n,y(x_n)) \tag{3.35}$$

The basic computational task is to advance the numerical solution to x_{n+1} after having computed $y_o, y_1, \ldots, y_n$. Any solution of equations (3.32) can be written as

$$y(x_{n+1}) = y(x_n) + \int_{x_n}^{x_{n+1}} y'(t)dt = y(x_n) + \int_{x_n}^{x_{n+1}} f(t,y(t))dt \tag{3.36}$$

The Adams method approximates this solution by replacing $f(t,y(t))$ with a polynomial, interpolating to computed derivative values, f_i, and then integrating the polynomial.

The Adams-Bashforth formula of order k at x_n uses a polynomial $P_{k,n}(x)$ interpolating the computed derivatives at the k preceding points,

$$P_{k,n}(x_{n+1-j}) = f_{n+1-j} \quad , \qquad j = 1,2,\ldots,k \tag{3.37}$$

These derivatives and y_n must be stored from the preceding step. An approximation to the solution at x_{n+1} is obtained from

$$y_{n+1} = y_n + \int_{x_n}^{x_{n+1}} P_{k,n}(t)dt \tag{3.38}$$

The algorithms we have used are based on the divided difference form of the interpolating polynomial.

We do now regard the Adams-Bashforth value y_{n+1} of equation (3.38) as a tentative, 'predicted' value and incorporate it into an interpolating polynomial. We rename the predicted value of equation (3.38) to p_{n+1} to avoid confusion. Using a new polynomial, $P^*_{k,n}(x)$, that also interpolates to k derivative values,

$$P^*_{k,n}(x_{n+1-j}) = f_{n+1-j} \,, \qquad j = 1,\ldots,k-1$$
$$P^*_{k,n}(x_{n+1}) = f(x_{n+1},p_{n+1}) \tag{3.39}$$

gives us the Adams-Moulton formula.

The approximate solution, y_{n+1}, is given by

$$y_{n+1} = y_n + \int_{x_n}^{x_{n+1}} P^*_{k,n}(t)dt \tag{3.40}$$

The algorithm we have used adjusts the order and step size to control the error per unit step in a generalized sense. The predictor-corrector approach is more accurate than most other known methods and therefore much better with respect to the propagation of error.

The reliability of the error estimates leads again to a more effective selection of the step size. A more detailed description of theory and algorithms can be found in Shampine and Allen (1973) and Shampine and Gordon (1975).

The numerical algorithms described above will also be used in integrating the Jacobian along the ray and the direction of vectors $\underline{e}_1$ and $\underline{e}_2$ (see Cerveny and Hron, 1980).

The integration of the wavefront curvatures must be performed together with the integration of the ray-tracing system and the vectors $\underline{e}_1$ and $\underline{e}_2$. This is due to the fact that we need to calculate the second derivatives of the velocity with respect to q_1 and q_2 (see for instance equation (3.30)) at points along the ray. Both $\underline{e}_1$, $\underline{e}_2$ and the position of the ray must be known in order to evaluate these derivatives. In the same way the integration of the Jacobian is dependent on the wavefront curvature. Thus, to perform the dynamic ray-tracing in a general model we need to integrate simultaneously 11, 12 or 15 equations depending on which of the systems (3.30), (3.31), (2.105), (2.111) or (2.118) are to be used. The functions y and f and the initial condition A in equation (3.32) are thus vectors with dimension 11, 12 or 15 in our case.

3.4 Intersection of ray and interface

In this section we shall shortly describe the special algorithm needed to find the point of intersection between the ray and the interface. In the case of a straight or circular ray and a plane interface this point may be found analytically. It is also possible to find the intersection point exactly if the ray is straight and the interface is a cylindrical cubic spline function as described in section 3.1. (In this case we must solve a cubic equation.) But, generally we need a search process to find this intersection point. We shall use a Newton algorithm, slightly modified from the one described in Gjøystdal (1979).

Let $\underline{x}$ be the coordinate of the ray and $\underline{t}$ the tangent vector at a certain time. The procedure could then schematically be described as follows:

i) If the vertical distance from $\underline{x}$ to the interface is less than a given limit, δ, initiate the Newton process.

ii) Find the point of the interface vertically below (or above) $\underline{x}$, here denoted $\underline{x}_I$, and compute a plane tangential to the interface at $\underline{x}_I$.

iii) Compute the intersection point between the tangent plane and a straight ray from $\underline{x}$ along $\underline{t}$ and store the distance, s, from $\underline{x}$ to the intersection point.

iv) Trace the ray from $\underline{x}$, a distance s to a new point $\underline{x}'$ with a new tangent vector $\underline{t}'$.

v) If the vertical distance from $\underline{x}'$ to the interface is less than a given limit, ε, we say that the intersection point is found.
If the vertical distance is greater than δ, stop the process.
Otherwise, define $\underline{x}$ as $\underline{x}'$, $\underline{t}$ as $\underline{t}'$ and go to ii).

If more than one intersection point has been found, choose the one, $\underline{x}_F$, corresponding to minimum tracing distance from the start point.

As soon as the intersection point is found, go back to the original ray point $\underline{x}$ (the one immediately before entering the Newton process) and continue going stepwise along the ray, each time checking if any interface is passed by the ray which for some reason has not been taken into account earlier. The tracing is stopped as soon as the last accepted intersection $\underline{x}_F$ is passed by the ray point $\underline{x}$.

The reason for going back to the ray point and continuing the stepwise procedure is that the geometry of the interfaces may in certain cases be such that we miss the proper interface the first time the Newton process is initiated. This may especially happen when the ray departs considerably from the vertical direction, so that the point $\underline{x}_I$ vertically below (above) the ray point $\underline{x}$ may be located relatively far from the proper intersection point. In such cases the interfaces may be so far from the ray point $\underline{x}$ that it is not included in the Newton algorithm the first time it is entered (see Fig. 3.3).

We have thus seen that the general problem of finding the intersection point between the ray and an interface may be solved by a numerical procedure, and that the solution generally will be accurate within certain predefined limits (dependent on the chosen value of ε).

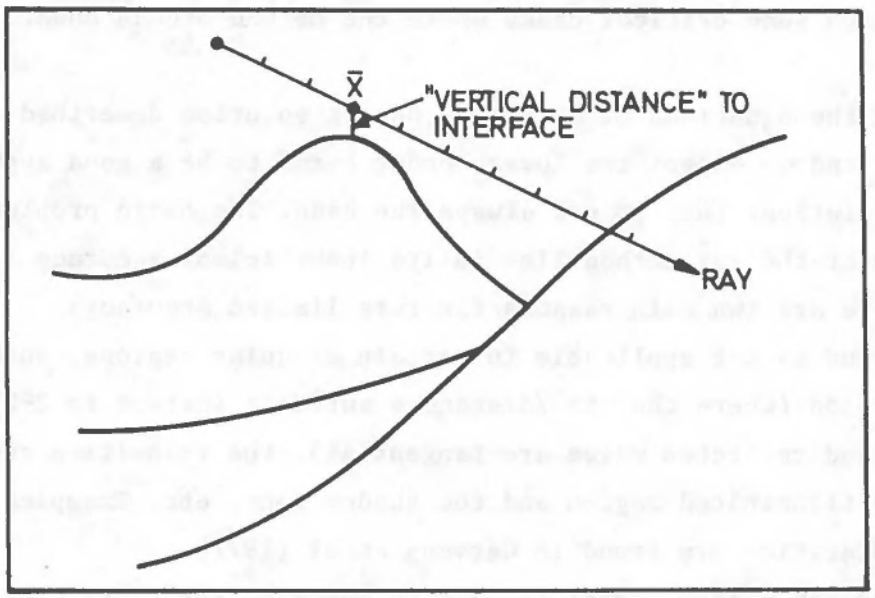

Fig. 3.3 Illustration of the ray/interface intersection process.

4. ERROR EVALUATION

4.1 Limitations on Theory

In this section we want to discuss some properties of the ray method and especially mention some critical cases where the method breaks down.

We have assumed the equations of motion to have a solution described in equation (2.5), and we expect the lowest order terms to be a good approximation to the solution. This is not always the case. The basic problem in the application of the ray method lies in its insufficient accuracy in certain situations. There are two main reasons for this limited accuracy:

i) The ray method is not applicable in certain singular regions, such as the critical region (where the time/distances surfaces (curves in 2-D) for head waves and reflected waves are tangential), the transition zone between the illuminated region and the shadow zone, etc. Examples of these singularities are found in Cerveny et al (1977).

ii) The standard ray method cannot be used to describe the properties of certain types of non-ray waves, such as various inhomogeneous waves, channel waves, tunnel waves, etc.

As an example of ii) we mention that the wave field does not behave according to the ray concept when there are serious changes in the medium perpendicular to the ray. In this case multiply reflected energy is generated, and the ray solution would be a modest approximation to the wave field. Even taking several higher order terms of the ray series into consideration will not do since we then still have assumed the ray concept to be valid (see Hudson, 1980, and Cerveny and Ravindra, 1973, for further references). We will try to avoid such critical models by smoothing the velocity function in the medium, but even in such models we may get problems at the interfaces. If the incident ray lies almost in the tangential plane of the interface we would have a situation like the one described above.

A modification of the ray method (see Cerveny, 1979A) makes it possible to use the method even in some of the singular regions mentioned above. Some of the non-ray waves mentioned could also be studied by the ray method using a complex eikonal (see Cerveny et al, 1977).

In more general terms we state that phenomena like diffraction and dispersion could not be modelled by using the standard ray series method. Contributions from diffraction curves in the medium could be calculated using a Kirchhoff-like integration (Berkhout, 1980) in addition to the ray series calculations.

When performing the tracing through interfaces we have implicitly assumed certain properties of the solution as we applied the phase matching method. Especially, head waves, i.e., waves propagating along the interface, do not obey the phase matching. Nevertheless, these waves can be modelled using the ray series. An exhaustive study of head waves is found in Cerveny and Ravindra (1973).

As it is shown in Cerveny et al (1977) the seismic rays are the extremals of the Fermat functional and according to the terminology of the calculus of variations the rays form the ray field in some region Ω if the two following conditions are fulfilled:

i) The rays cover the region Ω without crossing one another, i.e., one and only one ray comes through every point of the region Ω at each time.

ii) There exists a system of analytical surfaces which are transversal to the rays in the region Ω.

These are thus sufficient conditions for using the ray method.

The second condition guarantees the existence of wavefronts. When the Jacobian, J, which relates the ray coordinates $[\tau, q_1, q_2]$ to the Cartesian coordinates, does not vanish at any point of the region Ω, the ray field is called regular in the region Ω. If the Jacobian vanishes at any point in Ω, then the ray field is called irregular. The regularity of the ray field is a necessary condition for the applicability of the ray method. When the Jacobian is zero, the geometrical spreading vanishes and all the ray formulas lose sense.

In a seismological context we could say, with a slight oversimplification, that the ray expansion is not valid in the vicinity of those points where the time-distance surface (curve in 2-D) of the wave has end points, cusps, tangent points with the travel time surface of another wave, or, generally, discontinuous derivatives. This situation exists, for instance, in the vicinity

of boundary rays (which separate the shadow zone from the illuminated one) or caustics and critical rays (where the time-distance surfaces of reflected and head waves are tangential to each other). At caustics, the Jacobian vanishes and therefore the ray field is irregular there. The computation of the wave field in the neighborhood of the caustic is now a well-understood problem. Various approximate methods can be used to compute the amplitude here. However, this is not generally the case in an irregular region where the problem of finding asymptotics of the wave field can be rather complicated. Several examples of rays propagating in critical regions are discussed in Cerveny et al (1977).

It is well-known that the finite number of terms in the asymptotic series gives a satisfactory approximation to the functions under investigation in the case that the magnitude of individual terms decreases (under certain constraints) within the increasing number of terms in the series. Investigating the individual terms will give some rough validity conditions under which the sum of the N first terms in the ray series can be used to compute the wave field under consideration (see Cerveny et al, 1973; Cerveny et al, 1977; Gough, 1980; and Woodhouse, 1975). The validity conditions of the ray method, derived in the way suggested above, are:

i) The wavelength λ must be considerably smaller than the other characteristic quantities of length dimension $\ell_j (j=1,2,\ldots,n)$ in the problem under study

$$\lambda \ll \ell_1, \ell_2, \ldots, \ell_n \qquad (4.1)$$

The characteristic quantities ℓ_j are radii of curvature of the boundaries, measures of the inhomogeneity of the medium (for instance $v/|\nabla v|$, where v is the velocity), thicknesses of layers, measures of spatial changes of density, impedance, radii of curvature, etc. Many authors state this as a high frequency condition. This is due to the fact that they use an asymptotic expansion in inverse powers of frequency, ω^{-1}, instead of in dimensionless ratios of a type λ/ℓ_j.

ii) A regularity of the ray field in the investigated region is a precondition for the applicability of the ray method. As we have stated before, the ray

method fails even in the vicinity of surfaces (curves/points) S along which the Jacobian vanishes. Let n be the distance from the surface (curve/point) S. Then this validity condition can be stated as follows:

$$n \gg \lambda \qquad (4.2)$$

iii) The ray method is not applicable when the length L of the ray path between the source and the receiver is too great. This is due to the integrations performed to estimate the terms of order greater than or equal to one and does not come into consideration if the first term (zeroth order) is a good approximation. The ray length condition is estimated by the theorem of mean value.

$$L \ll \ell_o^2/\lambda \qquad (4.3)$$

Here ℓ_o has usually the meaning of measure of inhomogeneity in the direction of propagation of the wave under consideration. The quantity ℓ_o has the dimension of length. For the determination of L it is not necessary to take into account those parts of the ray path which are situated in a homogeneous layer between boundaries.

In Cerveny (1979A) several comparisons of the ray method with the reflectivity method (Fuchs and Müller, 1971) are made. Only the zeroth order term in the ray series is used, but some modifications are applied in the critical regions. The comparisons show that the ray method is of good quality even in some of the critical regions. Only two-dimensional models were used.

Several attempts to calculate the higher order terms in the ray series have been made. Cerveny et al (1973) uses polynomial Hilbert pairs of functions (see equations (2.6 & 7)) to estimate these terms. Woodhouse (1975) suggests a time integration method to calculate terms in the ray series beyond the first. L. Mark and F. Hron have studied the importance of the second term in the ray series for different models (Gough, 1980). It was found that in the majority of cases encountered in crustal seismology the magnitude of the

second term in the ray series is less than 8% of the leading term. For exploration seismology the significance of the second term is even smaller being generally in the range of 1%-5% of the leading term. Since these numerical results are the first ever reported, they represent a stepping stone in future studies concerning the accuracy of seismic numerical modelling.

4.2 Numerical errors

The numerical errors arise from one of the following sources:

i) Numerical integration of the differential equations

ii) Almost straight rays in the case of constant velocity gradient

iii) Model representation

iv) Newton search procedure.

The routines used to perform numerical integration require a local error tolerance as input. The steplength is then chosen automatically to fulfill this requirement. The computer representation of floating point numbers sets a lower limit on the local relative error to be given as input. For an IBM 4341 the lower limits are

single word representation	10^{-5}
double precision representation	10^{-12}

(These figures are approximate, and intended to give an impression of the orders of magnitude.) The relation between the local and the global error is discussed in Shampine and Gordon (1975). They conclude that except for very rare cases the global error can be estimated to within an order of magnitude off the local error. Thus, if we specify the relative local error tolerance to be 10^{-12}, we may expect the relative global error to be less than 10^{-11}. We have chosen to run our programs in a double precision representation to be sure that the global error in the integration is small enough.

We have run several tests to compare the integration algorithm with the analytical solution of the equations in the case of constant velocity gradient. For all models tested the ray paths and the tangential vectors approximate the solution at a relative accuracy of 10^{-11} when run in a double precision mode and demanding the relative local error to be less than 10^{-12}. However, we found that the relative global error in wavefront curvatures and in the Jacobian, in some cases could be 10^{-9} (three orders of magnitude off the relative local error). Likewise specifying a relative local error of 10^{-8}

gave a relative global error up to 10^{-5}. This was the case for all the five sets of equations (3.30), (3.31), (2.105), (2.111) and (2.118). All these equations depend on the evaluation of the ray paths, and therefore it is reasonable to assume that the increase in the relative global error for the wavefront curvatures is due to a reinforcement of the errors already introduced in the ray path evaluations. To test this hypothesis we traced some rays parallel to the velocity gradient (straight rays). In these cases the relative global error of the ray paths was the same as the requested relative local error and as we expected the relative global error of the wavefront curvatures was now not more than one order of magnitude off the relative local error. We did not test out this hypothesis to any further degree, since the relative global error still was bounded.

We found that all equations (3.30), (3.31), (2.105), (2.111) and (2.118) were compatible with respect to propagation of error, but for equations (2.118) and (3.30) we ran into problems satisfying the local error limit without using unreasonably small step sizes in the vicinity of irregular regions and in the source neighborhood. This is what we should expect since these two sets of equations are singular in these regions.

As far as the computer time is concerned, equations (3.30) and (3.31) seem to be the faster compared to (2.105), (2.111) and (2.118). Equations (3.31) are the faster in the vicinity of the source because the algorithm does not need an excessive number of steps to perform the integration in this area. Likewise approaching plane waves means that equations (3.30) are the best suited. We have used equations (3.31) in the vicinity of the source. Elsewhere we have used equations (3.30). In this way the algorithm will give us a flag when running into irregular regions where unreasonably small step sizes are needed. This is very important since the standard ray method is not applicable in irregular regions. The flag initiates a modification of the ray method taking into consideration the frequency dependence of amplitude and phase shifts of the reflected wave in this region (see Cerveny et al, 1977). This modification may be used in the vicinity of caustics, but it is not applicable in irregular regions in general (see section 4.1).

We have thus found that the error tied to the numerical integration of the differential equations is under control. On the basis of the testing of the algorithms we conclude that the relative local error tolerance can be set to 10^{-8} to be sure that the relative global error is significantly less than 10^{-3} or 1 o/oo. It is of great importance for the efficiency of the tracing that the error tolerances are defined not too strictly.

In sections 2.10 and 3.4 we described two different analytical solutions in the case of constant velocity gradient depending on whether the velocity gradient (∇v) and the tangent vector of the ray ($\underline{t}$) were parallel or not. During the numerical implementation and testing of these formulas we found that problems occurred when ∇v was 'almost' parallel to $\underline{t}$. In these cases ρ (the radius of curvature of the ray) in equation (2.84) turned to infinity. We have chosen to trace the ray as if $\nabla v \| \underline{t}$ (as a straight ray) when ρ exceeds a certain limit. We defined the limit in such a way that the error caused by this approximation was considerably smaller than the other errors involved in the ray tracing procedure.

The representation of the model (interfaces, velocities and densities) could be erroneous compared to the real model we want to represent due to the spline approximation. This is not a problematic error since the sampling interval in space could be made as small as we want, to make the spline functions approximate the real model within any error limit down to the representation limit of floating points in the computer.

As we have described earlier we seek the intersection points between the ray and any interface using a Newton algorithm. At every point of intersection we will thus introduce an error due to the specified tolerance of the Newton iteration. Since we have control with this tolerance, we can make this error as small as we want down to the accuracy of the computer.

In most applications a relative global error less than 0.001 or 1 o/oo would be considered a good result. As we have seen above, there is no problem in determining the tracing time and distance, the wavefront curvatures and the Jacobian within this limit. From the considerations above we thus conclude that there is no problem in making the numerical error significantly less than the error associated with truncating the ray series after the first term, and thus that the ray series approach can be successfully used in a numerical procedure to perform dynamic ray tracing.

5. SYNTHETIC SEISMOGRAMS

5.1 Theoretical considerations

The main application of the theory developed in this thesis will be the construction of synthetic seismograms. That is: Given a source position and an array of receivers distributed along a curve, constuct a seismogram for each receiver taking into consideration contributions from a prespecified number of interfaces, primary reflections as well as multiples.

The main complication in doing the synthetics is connected with the fact that the computation of the ray path is not a Cauchy initial value problem, but a two-point boundary value problem (since we are looking for the ray connecting the source with a given receiver). The solution of a two-point boundary value problem is usually easier when the distance between source and receiver is small (see Cerveny, 1979B). Due to the model complexity, the travel-time surfaces (curves in 2-D) of important waves may have several branches at larger distances, and we must determine all of them.

Methods for solving the two-point ray-tracing problem are discussed for instance in Julian and Gubbins (1977). Two methods are considered: the shooting method and the bending method. The shooting method involves integrating the initial value formulation of the problem, and employing a procedure for finding the starting direction which yields the desired ray. The other method involves taking some initial estimate of the ray path and perturbing it, while keeping the ends fixed, until the true ray is found. This is essentially a variational approach. The differential equations for the ray are expressed in terms of changes in the ray path and linearized, and the resulting equations are solved by the finite-difference method. This involves the solution of a system of linear algebraic equations. As with the shooting method, the procedure must be applied iteratively, because the ray equations are nonlinear. To derive the differential equations of the ray, Fermat's principle of stationarity of travel time with respect to small path variations, is applied. This will not be valid in some cases of complicated geological structures (faults, intersection of interfaces, etc.). For this reason the bending method is not the best suited for our use.

The main problem in using the shooting method is to find a reliable and efficient procedure for finding the starting direction which yields the desired ray. We will base our work on the ZCS-method described in Gjøystdal (1978A & 1978B). This is a general search procedure for sampling of zero-value contours of a bivariate scalar function.

5.2 Problem formulation

Let $\underline{p_o}$ be an initial ray parameter vector, that is, a vector consisting of both initial position coordinate and initial tangent vector. Further, let ℓ be a given receiver curve along which all receivers are distributed. This curve is represented by a cubic spline function defined in a coordinate system $x_1'x_2'$ called the receiver-line system as shown in Fig. 5.1. Thus ℓ is supposed to be a function of x_1', $\ell = \ell(x_1')$.

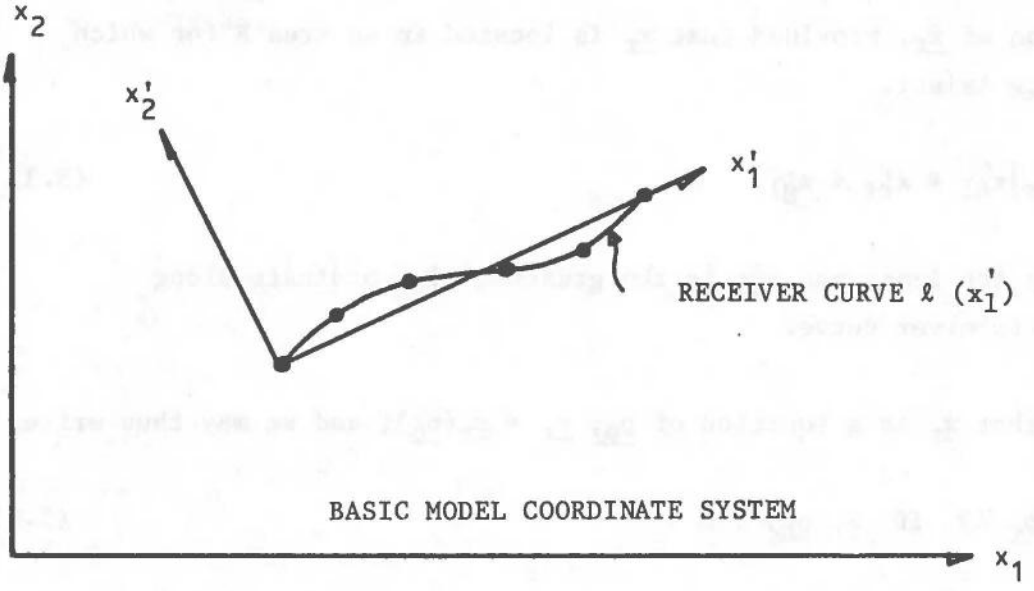

Fig. 5.1 Receiver curve represented by a cubic spline function.

We shall be interested in a family of rays emerging from a source point $\underline{x}_s$ and arriving on (or very close to) the line ℓ in such a way that samples are obtained along all parts of ℓ where arrivals are possible. The density of the samples should be good enough to make possible a satisfactory interpolated equidistant sampling along ℓ at a later stage. We shall assume that ℓ lies in an interface (f.ex., the model surface) to which the rays shall be traced. Denoting the coordinates of the arrival point by

$$\underline{x}_r = (x_{r1}, x_{r2}, x_{r3}) \tag{5.1}$$

we define the 'horizontal distance' from $\underline{x}_r$ to ℓ by the expression

$$d = d(\underline{x}_r | \ell) = x'_{r2} - \ell(x'_{r1}), \quad \underline{x}_r \in R \tag{5.2}$$

where x'_{r1} and x'_{r2} are the coordinates of the arrival point $\underline{x}_r$ relative to the 'receiver line system' $x'_1 x'_2$. With 'distance' we simply mean difference between the x'_2-coordinates. The distance d is expressed as a function of $\underline{x}_r$, provided that $\underline{x}_r$ is located in an area R for which this distance exists.

$$R = \{\underline{x}_r | x'_{\ell 1} \leq x'_{r1} \leq x'_{g1}\} \tag{5.3}$$

where $x'_{\ell 1}$ is the least and x'_{g1} is the greatest x'_1-coordinate along the defined receiver curve.

We observe that $\underline{x}_r$ is a function of $\underline{p}_o$, $\underline{x}_r = \underline{x}_r(\underline{p}_o)$, and we may thus write

$$d = d(\underline{p}_o | \ell) \quad \text{if} \quad \underline{x}_r(\underline{p}_o) \in R \tag{5.4}$$

We now proceed to find initial ray parameter vectors $\underline{p_o}$ satisfying the requirement

$$|d(\underline{p_o})| < \varepsilon \tag{5.5}$$

in order to compute ray paths arriving closer to the receiver line than a given $\varepsilon > 0$.

It is easy to see that just two of the six components of $\underline{p_o}$ are undetermined. The initial coordinates are given, and one of the components of the tangential vector is dependent on the two others since the tangential vector is claimed to be a unit vector. We can thus reduce the problem to a search for <u>two</u> initial ray paramters (p_1, p_2), which could for instance be horizontal components of the initial unit tangent vector, such that

$$|d(p_1, p_2)| < \varepsilon \tag{5.6}$$

We will now describe this 'two-parameter search algorithm' to be used for this problem.

5.3 Algorithm description

Assume that a scalar function of two variables is defined on a region S of the x_1x_2-plane

$$y = f(\underline{x}), \qquad \underline{x} \in S \tag{5.7}$$

where $\underline{x} = (x_1, x_2)$ is a vector notation for the independent variables.

Assume further that S may be divided into regions S_i, i=1,...,n in such a way that f is continuous on each S_i (that is, f is piecewise continuous on S).

The method to be described in this section was designed in order to calculate solutions of the equation

$$f(\underline{x}) = 0 \tag{5.8}$$

provided that such solutions exist somewhere in S. The procedure is based on the assumption that the following two operations are available:

Given an arbitrary point $\underline{x}$
(i) Determine if $\underline{x} \in S$
(ii) If $\underline{x} \in S$, find $f(\underline{x})$.

Geometrically, the calculation of solutions of (5.8) corresponds to determination of intersection curves (or tangential curves) between the surface $y = f(\underline{x})$ and the $\underline{x}$-plane. In special cases one may think of having $f = 0$ in whole regions of the $\underline{x}$-plane, however, our method will be restricted to cases in which the solutions are made up of one or more continuous curves in S. Our aim will be to sample these curves (in the following denoted by C) in a given number of points, i.e., to calculate solutions of the form

$$\underline{x}_{ij}, \qquad i=1,N_j, \quad j=1,M \tag{5.9}$$

Here $\underline{x}_{ij}$ denotes sample point no. i of the j-th curve C_j, N_j is the number of samples for C_j and M the total number of separate curves.

It should be noted that in the numerical procedure, equation (5.8) must be replaced by the requirement

$$|f(\underline{x})| < \varepsilon \tag{5.10}$$

i.e., a point $\underline{x}$ is a satisfactory solution when giving functional values closer to zero than a certain predefined limit.

The method may be described as follows. We start with a certain set of initial values

$$\underline{x}_i, \qquad i=1,\ldots,N_g \tag{5.11}$$

and select those $\underline{x}_i$ satisfying

$$|f(\underline{x}_i)| < \varepsilon_g \tag{5.12}$$

where ε_g is some preselected positive value. Thus we obtain a set of initial points $\underline{x}_i$ giving functional values in a 'reasonable vicinity' of zero. Then, by calculating ∇f numerically, we search along the direction of the gradient (in + or - direction depending on the sign of f) and thereby displace the points $\underline{x}_i$ into new positions lying on (or sufficiently close to) the C-curves, so that

$$|f(\underline{x}_i)| < \varepsilon \tag{5.13}$$

Finally, by starting in one of these displaced points, we search in directions normal to the gradient (i.e., along the tangent of the C-curves) and perform a sampling of the C-curves corresponding to the specified receiver points. As soon as a C-curve has been sampled, we go through the remaining start points $\underline{x}_i$ and skip those which happen to belong to the C-curve just found. By choosing the initial grid dense enough, we can, at least in principle, be sure of 'catching' all branches of the C-curves existing within the region S.

5.4 Numerical examples

We will now present synthetic seismograms for a number of different models. All amplitude calculations are for P-waves only. Our first model is a simple 1-D model described by 4 homogeneous horizontal layers. The velocity between the surface and the first interface is 1.5 km/s. (The interfaces and layers are numbered from the surface and downwards. The surface is not counted as an interface.) In the next layers the velocities are 2.0, 2.5 and 3.0 km/s, respectively. The velocity below the fourth interface is 3.5 km/s. We let the density be the same constant value in all layers. The model coordinate

system has x and y coordinates in the surface plane both ranging from 0.0 to 4.0 km. The plane interfaces are positioned at depths of 1.0, 2.0, 3.0 and 4.0 km, respectively.

The first synthetic section to be generated from this model is presented in Fig. 5.2. This is a single shot section. The signal is sent from the surface at (1.,2.) and the receivers are distributed along a straight line from (1.,2.) to (2.8,2.) equally spaced. The pulse shape is a typical seismic reflection signal which is recorded from shots in ore mines. This pulse shape will be used in the following sections.

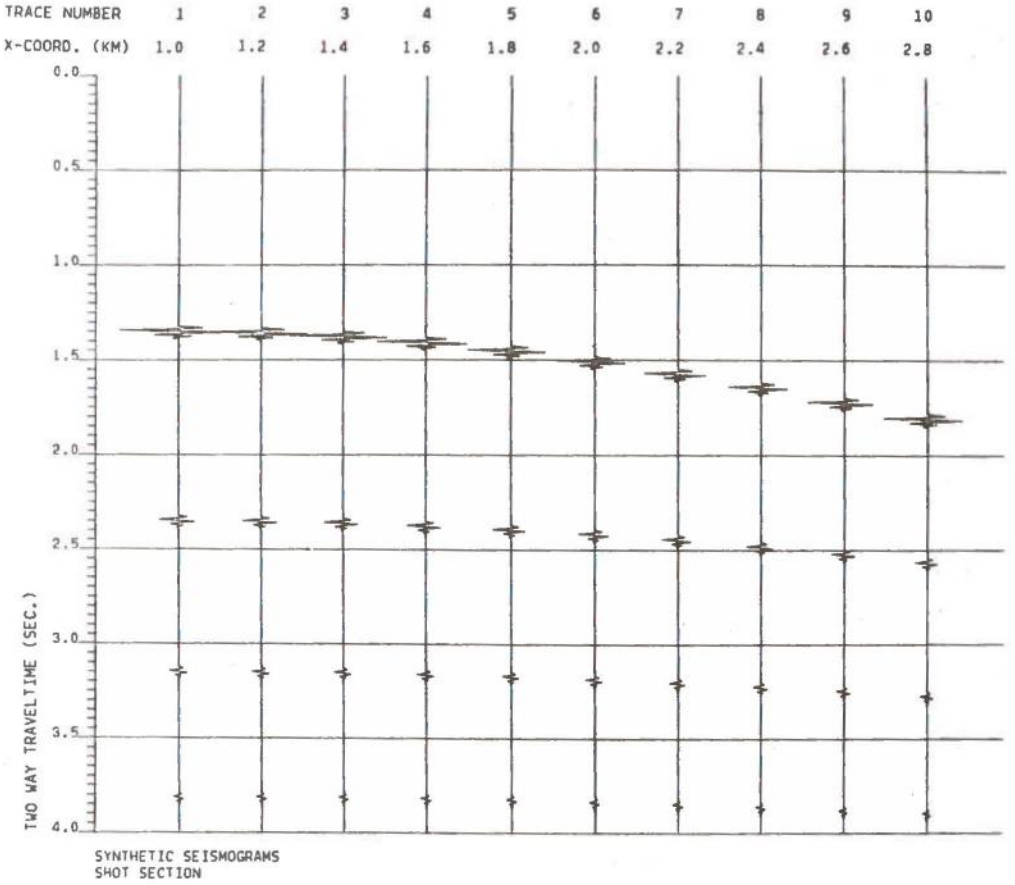

Fig. 5.2 Single shot section for a model with four homogeneous horizontal layers.

The ray paths are as plotted in Fig. 5.3.

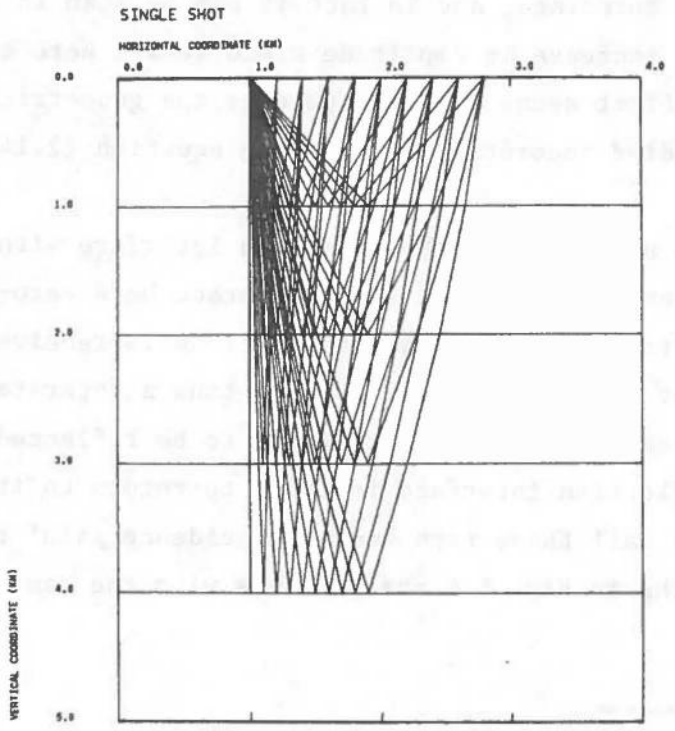

Fig. 5.3 Ray paths of a single shot section with 10 receivers. Vertical cross-section of the model along the shot/receiver line.

We clearly observe (in Fig. 5.2) the hyperbolas formed by the arrivals from the different layers due to the offset of source and receivers. This effect is called the move out effect and is easily compensated for in the case of horizontal layers by the standard normal move out (NMO) formula (Taner and Koehler, 1969). The reason for doing this correction is to simplify the interpretation of the section. The purpose is to have the section look as if each trace is shot and received at the same point. In a more complex model these corrections get complicated. In general there exists no analytic formula to correct for the NMO effect. As we observe, the hyperbolas get less curved as reflected from the deeper reflectors since the offset is relatively smaller compared to the length of the ray paths for these reflections.

We also observe that the signal reflected from the three deepest interfaces decreases in amplitude with increasing x-value. This is due to the geometrical spreading (rays with the greatest offsets have the longest ray paths). Of course, this effect should also be observed in the signals reflected from the first interface, and in fact it can be seen in traces 1 to 8. The two last traces increase in amplitude since we are here close to total reflection, and this effect seems to dominate over the geometrical spreading. This effect may be studied theoretically by using equation (2.143).

In the following we do not want the NMO effect to interfere with other effects to be studied and therefore we let each trace be a zero-offset trace. That is, every trace in the following sections is received in the same point as where the signal is sent from, and thus a separate signal is sent and received for each trace. Each ray needs to be reflected in a direction normal to the reflection interface in order to return to its initial position. We therefore call these rays 'normal incidence path' rays or just NIP rays. The ray paths in Fig. 5.4 are NIP rays with the same receivers as used in Fig. 5.3.

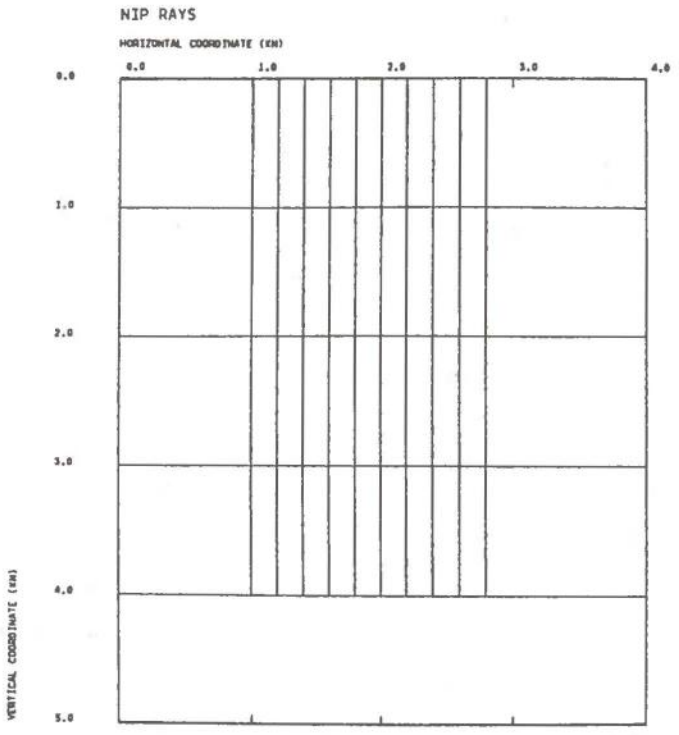

Fig. 5.4 NIP rays for a model with homogeneous layers and horizontal interfaces.

Our first section in Fig. 5.2 would in this case be as in Fig. 5.5.

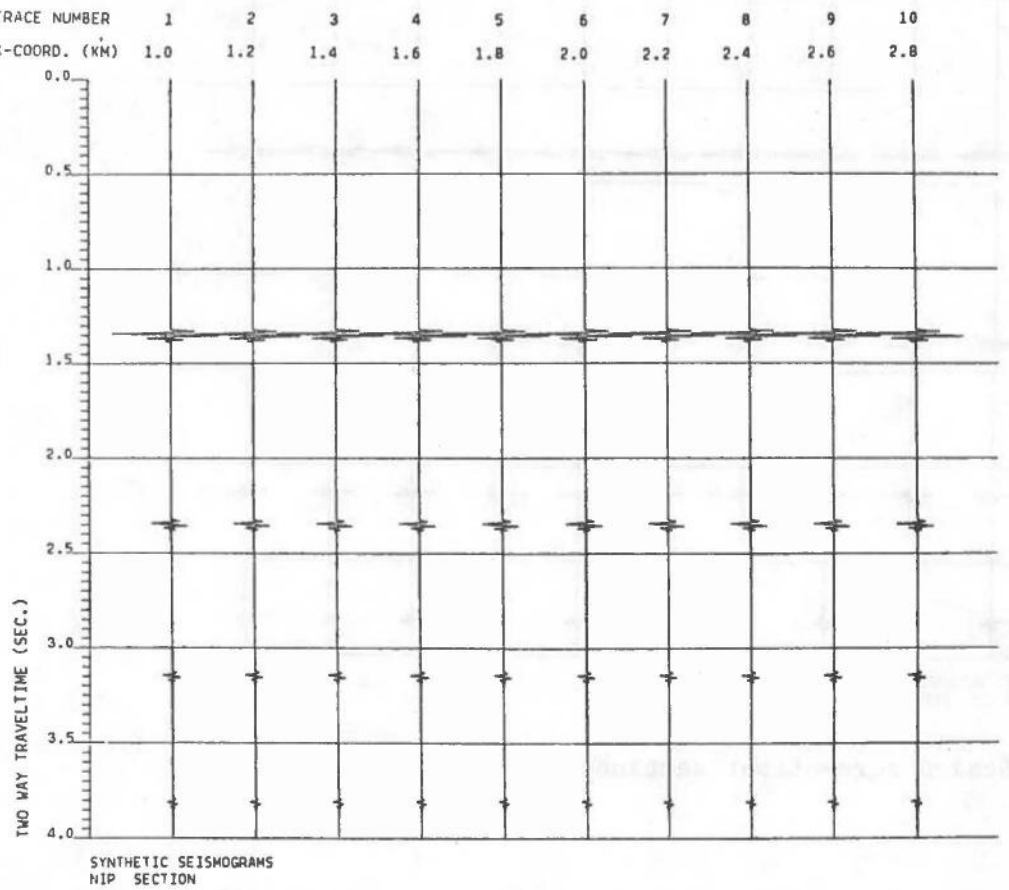

Fig. 5.5 A zero-offset section for a model with homogeneous layers and horizontal interfaces.

As we observe, the reflections from the deepest interfaces are weak compared to the first arrivals. To compensate for the large dynamic range of the arrivals, we may scale each trace by multiplying the amplitude value at each time by a constant multiplied by the time itself. Since this scaling is the same for each trace, we still have the possibility to compare amplitudes arriving at the same time in different positions. Fig. 5.6 shows this scaling applied on the zero-offset section in Fig. 5.4.

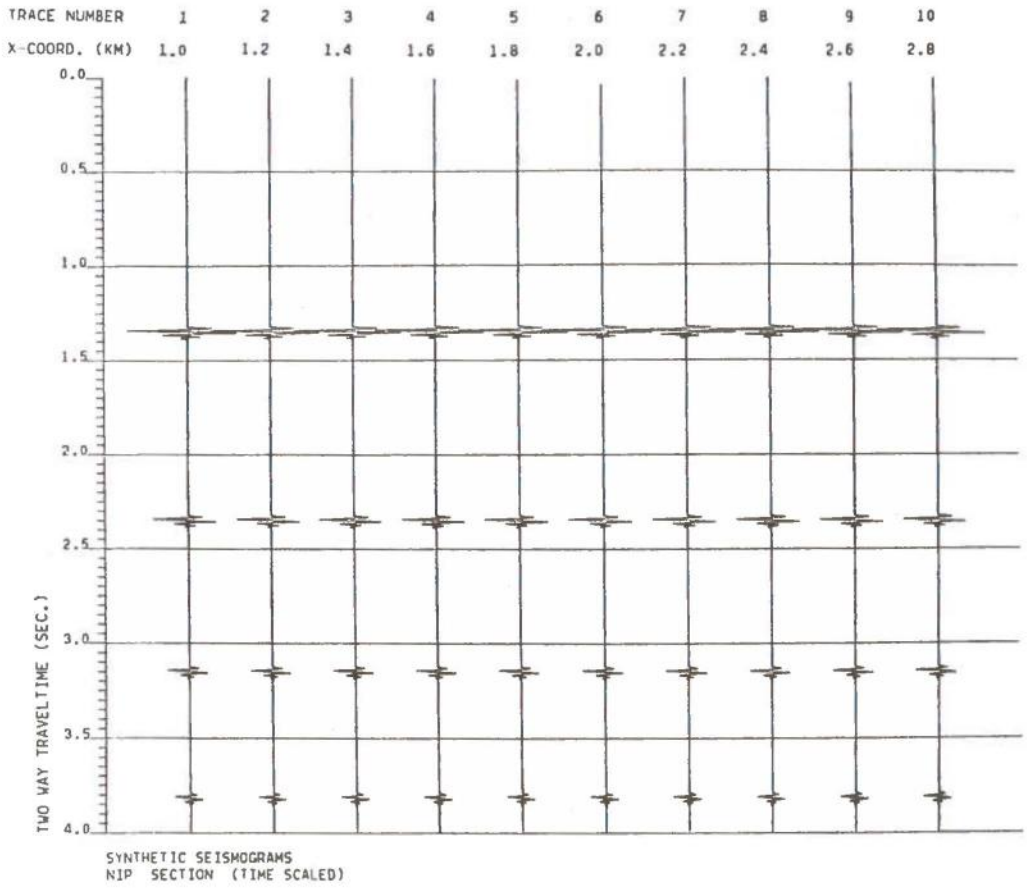

Fig. 5.6 Scaled zero-offset section.

The scaling is a rough correction for the geometrical spreading. As we know, the amplitude decrease is proportional to the inverse distance between source and receiver in the case of a homogeneous medium. In the following this time-scaling will be used.

We will now generalize this model by letting the velocity vary continuously within each layer. To maintain the possibility of displaying the rays in 2 dimensions, we let the velocity be described as

$$v_3(x,y,z) = 2.1 + 0.1x + 0.2z$$

in the third layer, and as

$$v_4(x,y,z) = 2.9 + 0.3x + 0.1z$$

in the fourth layer. The medium below the fourth layer has velocity

$$v_5(x,y,z) = 3.8 + 0.3x$$

All velocities are given in km/s. The other parameters describing the medium remain as before. We let the shot/receiver positions be along the same line as before but our first trace will now be in (0.5,2.0) and the rest equally spaced with 0.3 km along the line up to (3.2,2.0). Fig. 5.7 shows the ray paths and Fig. 5.8 shows the synthetic zero-offset section.

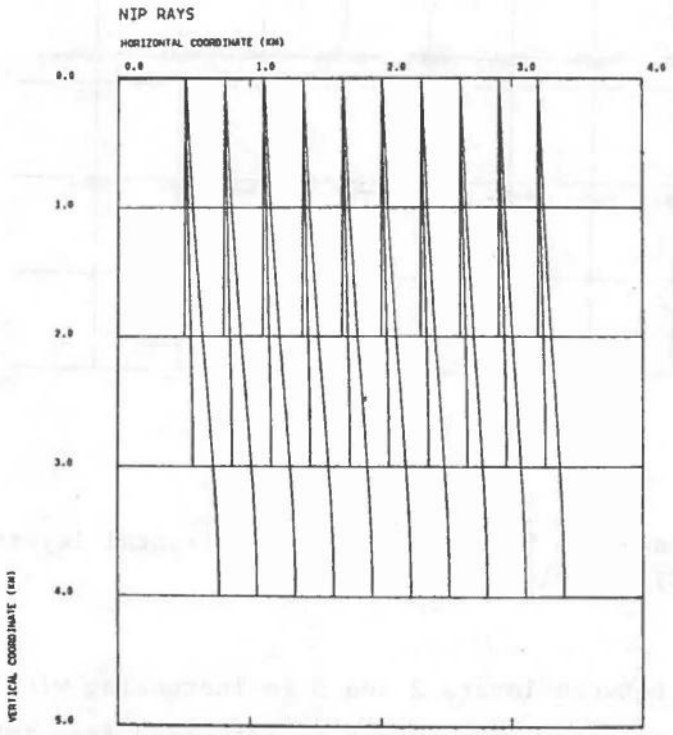

Fig. 5.7 Ray paths in a linearly varying medium. Vertical cross-section of the model along the shot/receiver line.

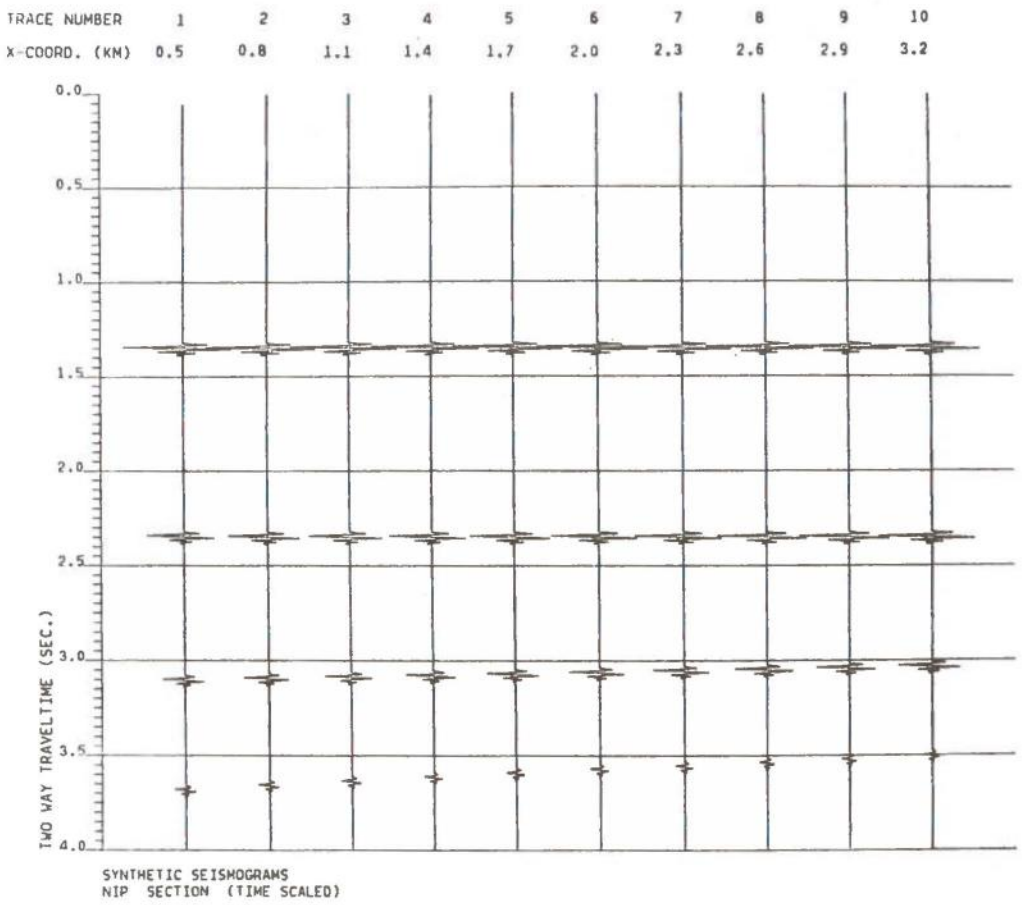

Fig. 5.8 Zero-offset section for a model with horizontal layers and linearly varying velocities.

The velocity contrast between layers 2 and 3 is increasing with increasing x-coordinate. As a consequence more energy is reflected from interface 2 as the x value increases. This is clearly observed in the seismograms. The same effect is observed in the reflections from interface 3. The amplitude of the signals from the fourth interface seems to decrease with increasing x. The interpretation of this must be that less energy is coming through to the deepest interface for high x values due to the increasing velocity contrast with x at the above-laying interfaces. We also observe

that since the velocity increases with x in layers 3 and 4, the arrivals from interfaces 3 and 4 are coming earlier for higher x-values.

We will now leave this model and start tracing in a more general 3-D model shown in Fig. 5.9.

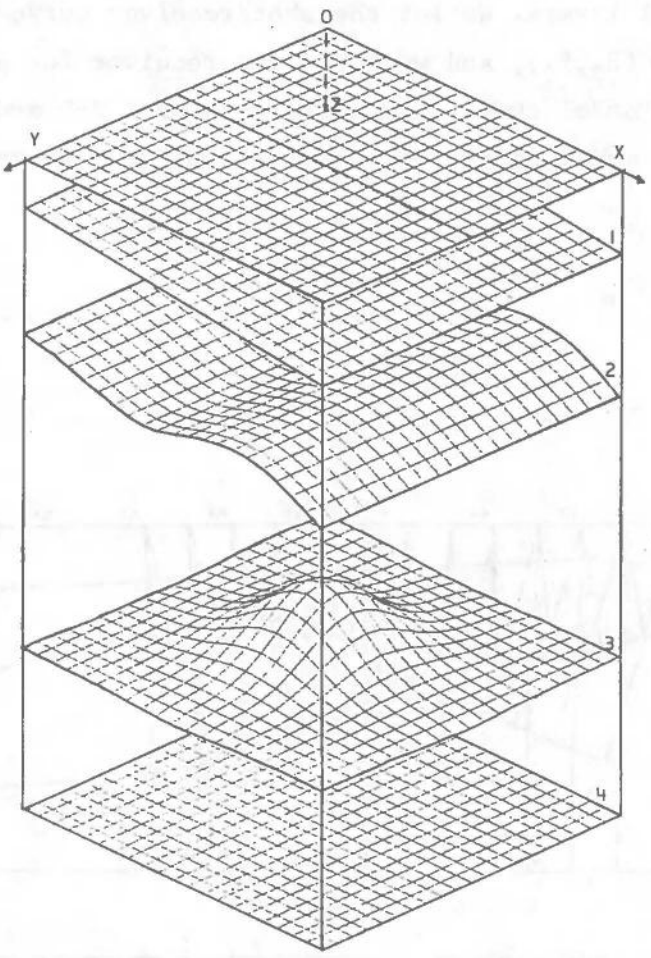

Fig. 5.9 Three-dimensional plot of the synthetic model. Vertical scale is exaggerated. Horizon extension is 10 x 10 km; vertical extension is 4 km.

It consists of four reflecting interfaces: (1) Plane dipping in the x-direction, (2) curved interface dependent only upon the x-coordinate (cylindrical spline surface), (3) generally curved interface (symmetrical around a vertical axis through surface point (5.,5.)), and (4) horizontal plane interface.

The velocities are given as 1.8 km/s in the first layer and 2.1, 2.5, 3.0 and 3.5 km/s in the following layers. The density will still be the same constant value in all layers. We let the shot/receiver curve be a straight line from (2.,5.) to (8.,5.), and we place one receiver for each 0.5 km. In this case our 3-D model could be treated as a pure 2-D model. A vertical cross section of the model along the shot/receiver line contains all ray paths.

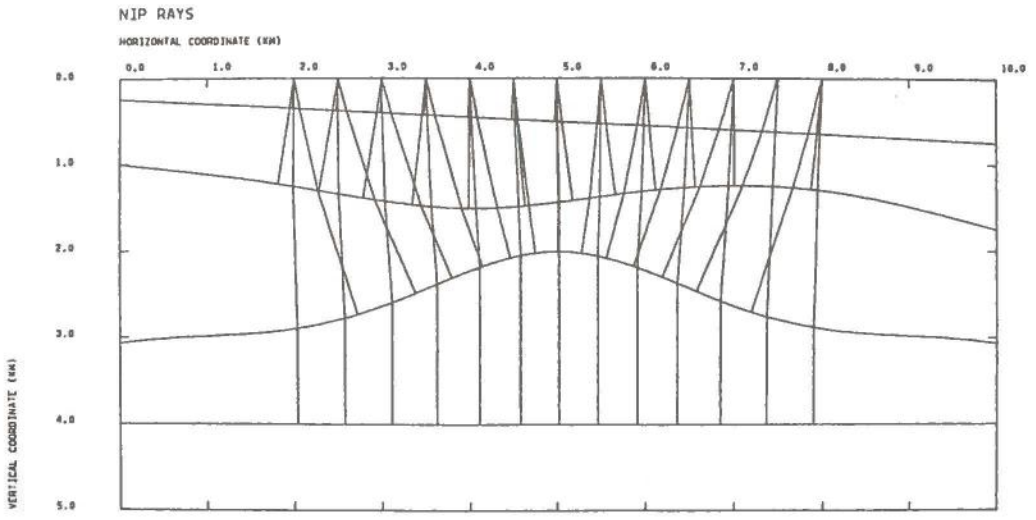

Fig. 5.10 Ray paths in a medium with constant velocities. Vertical cross section of the model along the shot/receiver line.

The synthetic seismograms are presented in Fig. 5.11.

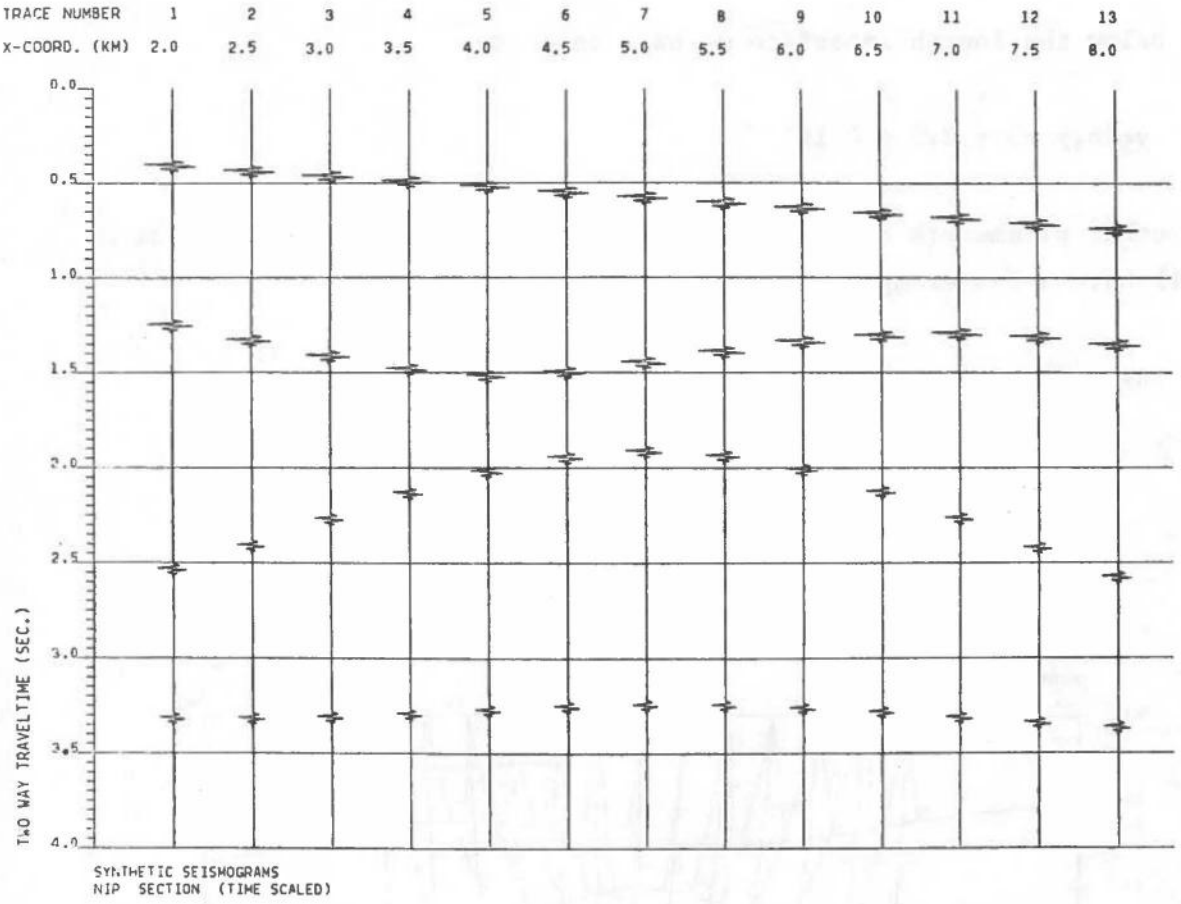

Fig. 5.11 A zero-offset section for a 2-D model with homogeneous layers and curved interfaces.

We clearly observe that the arrivals from the fourth interface do not line up due to the lense effects of the overlaying layers.

The next synthetic section to be presented is shot and received in the same positions as the previous one, but the velocity structure in the layers is slightly different. In the first layer the velocity is still constant, 1.5 km/s. For the next layers the velocities are

$$v_2(x,y,z) = 1.8 + 0.01x + 0.1z$$
$$v_3(x,y,z) = 2.5 + 0.01x + 0.001z^2$$
$$v_4(x,y,z) = 3.0 + 0.01x + 0.3z$$

and below the fourth interface we have velocity

$$v_5(x,y,z) = 3.5 + 0.1x$$

All other parameters remain as in the the previous example, and thus we still have a 2-D example.

The ray paths are shown in Fig. 5.12.

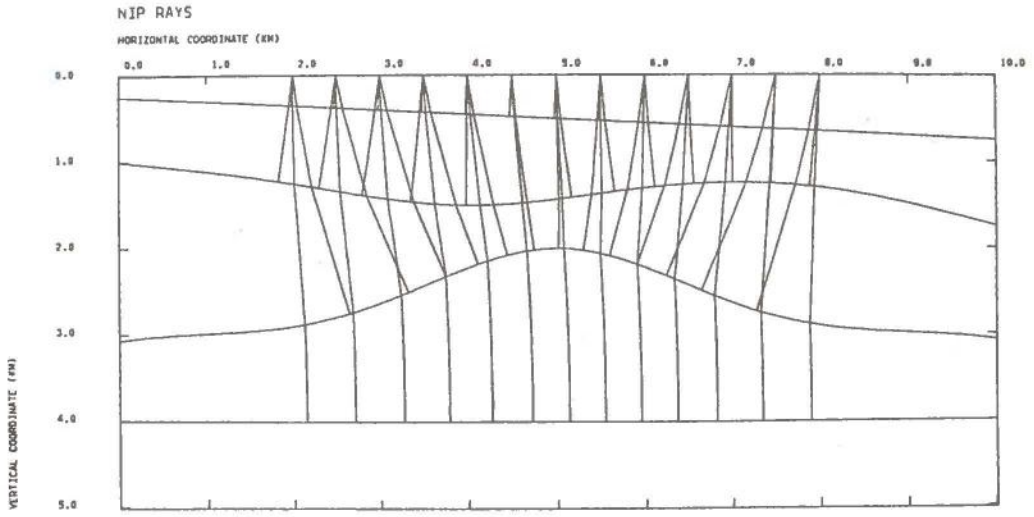

Fig. 5.12 Ray paths plotted in a vertical cross section of the model along the shot/receiver line.

We observe that the ray pattern is very much like the one in the previous example. This is mainly due to the fact that the velocity gradients are relatively small. However, by a closer look at Fig. 5.12 it is still possible to see that the rays in layer 4 are somewhat curved. In layers 2 and 3 the gradients are particularly small and the rays seem therefore almost straight plotted in this scale. The synthetic seismograms of this section are shown in Fig. 5.13.

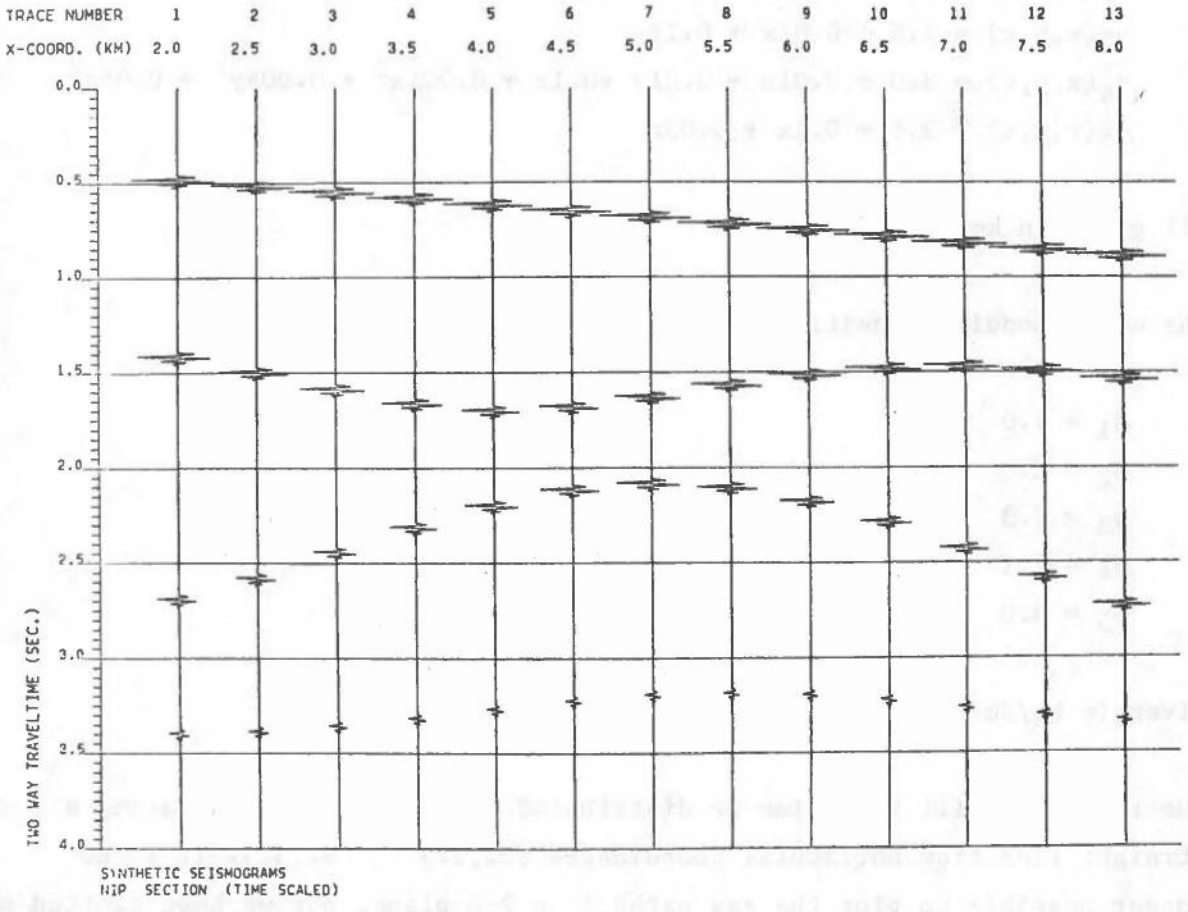

Fig. 5.13 A zero offset section for a 2-D model with curved interfaces and continuously varying velocities.

The section resembles the one plotted in Fig. 5.11, but it is a bit more difficult to reconstruct the model structure on the basis of the seismograms in Fig. 5.13. Also the amplitude pattern has changed from Fig. 5.11 due to the change in velocity structure.

Finally we present an example of a general 3-D dynamic ray-tracing. The interfaces are still as presented in Fig. 5.9, and the velocities in the layers, listed from the surface and downwards, are as follows:

$$v_1(x,y,z) = 1.7$$
$$v_2(x,y,z) = 1.8 + 0.3x + 0.1y + 0.1z$$
$$v_3(x,y,z) = 2.5 + 0.01x + 0.1z$$
$$v_4(x,y,z) = 3.0 + 0.01x + 0.01y + 0.1z + 0.001x^2 + 0.004y^2 + 0.05z^2$$
$$v_5(x,y,z) = 3.5 + 0.1x + 0.03z$$

all given in km/s.

The corresponding densities will be

$$\rho_1 = 1.0$$
$$\rho_2 = 2.0$$
$$\rho_3 = 2.3$$
$$\rho_4 = 2.1$$
$$\rho_5 = 3.0$$

given in kg/dm^3.

The receivers will this time be distributed with 0.5 km spacing along a straight line from horizontal coordinates (2.,2.) to (9.,5.). It is no longer possible to plot the ray paths in a 2-D plane, but we have plotted a vertical cross section of the model along the receiver line. The plotted ray paths are projections of the real rays into the plotted cross section.

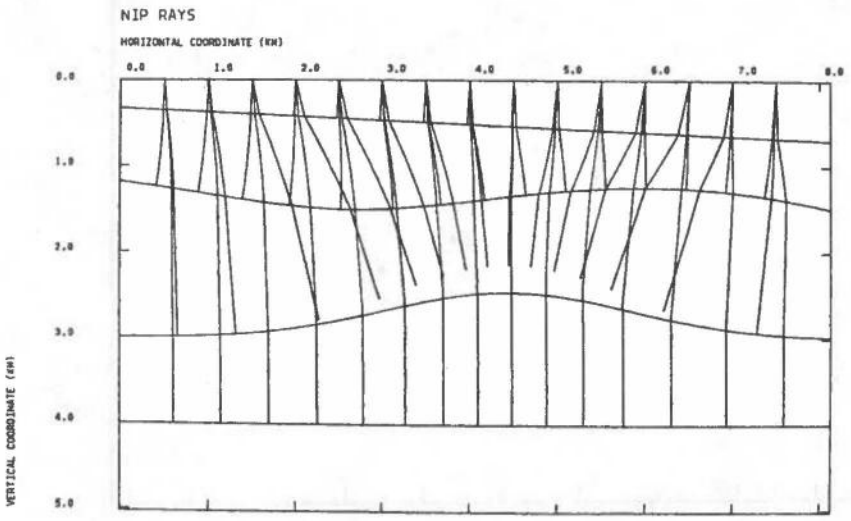

Fig. 5.14 Vertical cross section of the model along the shot/receiver line. Horizontal coordinate 0.5 km is at position (2.,2.).

We clearly see that the rays reflected from the third interface are not reflected from points in this cross section of the model. The reflection points (or NIP foot points) are plotted in Figs. 5.15 to 5.18 in horizontal coordinates. We observe that most of the NIP foot points do not lie on the straight line from (2.,2.) to (9.,5.).

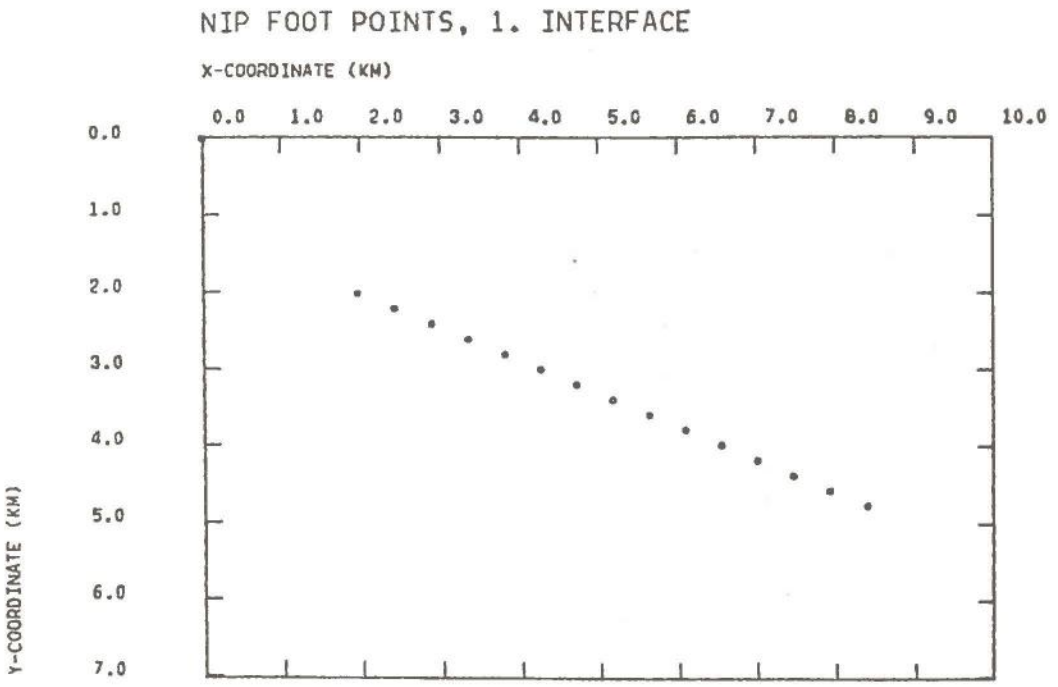

Fig. 5.15 Reflection points for rays reflected at the first interface.

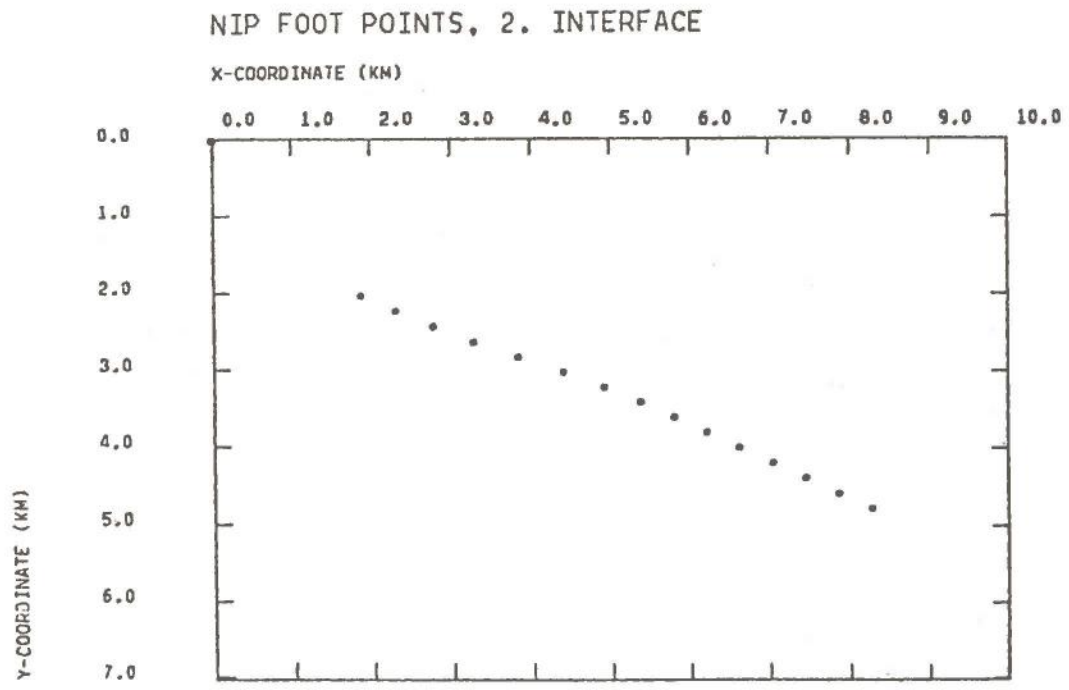

Fig. 5.16 Reflection points for rays reflected at the second interface.

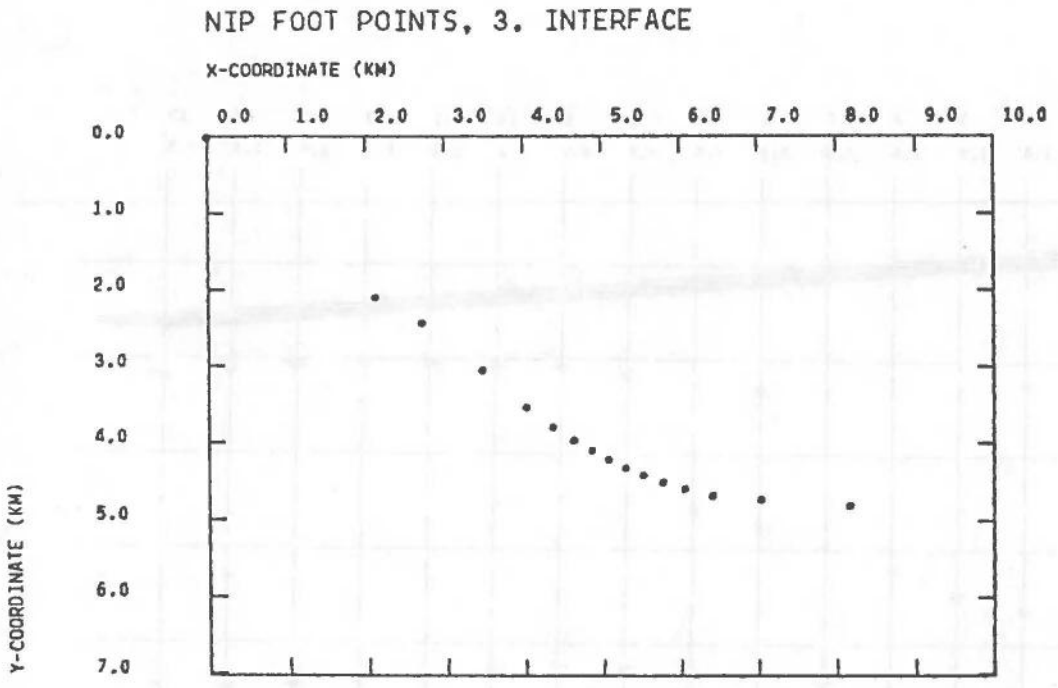

Fig. 5.17 Reflection points for rays reflected at the third interface.

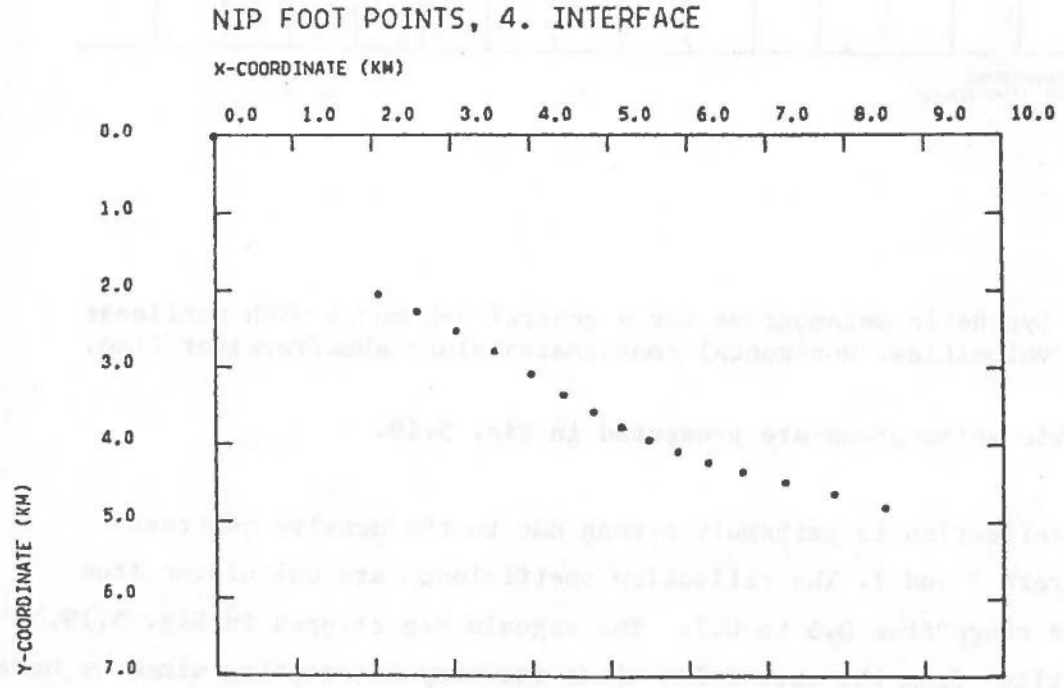

Fig. 5.18 Reflection points for rays reflected at the fourth interface.

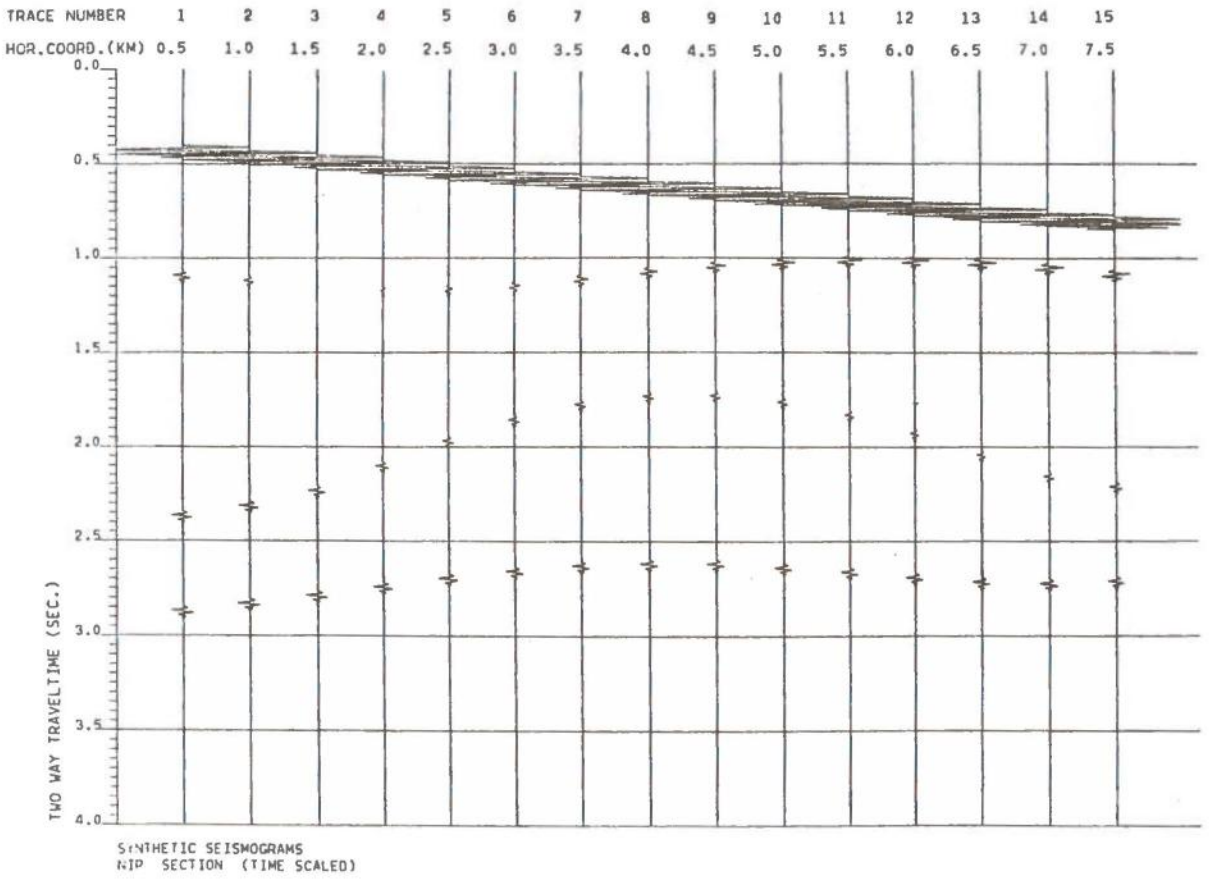

Fig. 5.19 Synthetic seismograms for a general 3-D model with nonlinear velocities. Horizontal coordinates along shot/receiver line.

The synthetic seismograms are presented in Fig. 5.19.

The first reflection is extremely strong due to the density contrast between layers 1 and 2. The reflection coefficients are calculated from (2.143) and range from 0.5 to 0.7. The signals are clipped in Fig. 5.19. The reflections from the second interface are very interesting since we here

observe a phase shift somewhere between traces 2 and 4. The reflection coefficients for these rays are negative in traces no. 4 to 15. We have calculated the reflection coefficients for traces no. 1, 3, 4 and 10 to be 0.06, 0.01, -0.03 and -0.15, respectively.

A comparison between the cross section in Fig. 5.14 and the section in Fig. 5.19 tells us that the overall structure of the model is maintained in the seismograms, but more detailed interpretations of the model structure are difficult to make.

6. CONCLUDING REMARKS - FUTURE DEVELOPMENTS

We have developed a general 3-D dynamic ray-tracing procedure for the construction of synthetic seismograms. The work has been based on adaptation and applications of recent developments in the field of dynamic ray tracing. Analytical solutions have been obtained whenever possible to make the algorithms fast. Different methods to solve the differential equations numerically have been considered. Our demands have been efficiency and still maintaining the global error at an acceptable level. We found that the Adam's PECE (Predict-Evaluate-Correct-Evaluate) method was best suited for our use.

The model interfaces might have any shape that could be modelled by using a set of spline functions.

Several representations of the velocity structure are also suggested, although we have not implemented a 3-D spline function for the most general case.

A Newton process was used to determine the intersection point between ray and interface and the accuracy could be made as good as requested.

The shooting method was applied to find rays connecting given source and receiver points. Provided the existence of such a physical ray, it may be determined within a prespecified accuracy.

We thus conclude that the numerical errors are under control and that most restrictions lie in the limitations of the theory. The fact that we have only used the first term of the amplitude coefficients in the ray series represents one of greatest errors in this respect. We have not tried to investigate the second term but some results have been referred. Still none of these works are exhaustive and much research remains to be done on this particular problem.

The irregular regions have already been investigated to a large extent in 2-D and simple 3-D models. We have not made any progress here, especially because no reference programs have been available to us for comparison.

However, programs constructing synthetic seismograms in general 3-D models based on other concepts than the ray method are now being developed at Bullard Laboratories, the University of Cambridge, United Kingdom, and it has been agreed to make comparisons as soon as possible.

It is well known that the application of the ray method to the construction of theoretical seismograms is best suited in the case of relatively 'short' distances between source and receiver (e.g., reflection methods in seismic prospecting). In this case, the construction of theoretical seismograms does not cause great difficulties and the accuracy of computations is usually quite satisfactory, even in the case of rather complicated structures. The thesis contains several examples of such seismograms. We have not tried to give advanced and exhaustive interpretations of these, but they are included to show some of the possibilities for the procedures developed. Many effects appearing in real seismograms may now be studied theoretically in a 3-D world. This includes ocean bottom multiples, peg-legs, side reflections, focusing effects, etc. The procedures are considered a well-suited tool for training exploration geophysicists in understanding the effects of various model features and thus a significant contribution to improved seismic interpretation.

Only P-waves have been considered so far, but an extension to include S-waves is straightforward. In this way the significance of S-waves in reflection seismograms may be studied.

We have at this stage not accounted for the impact of the receiver instrument (seismometer/hydrophone/geophone) and the free surface at the receiver position. This is necessary in order to make a comparison between real and synthetic seismograms.

Also the source functions could be improved. In the results presented we have simply used a point source.

Finally it is to be stressed that this is a pure geometrical approach to the construction of synthetic seismograms and that the attenuation effects due to frictional loss in the medium has not been included.

As far as the future developments are concerned, we want to mention three items in particular. The first one is the use of the dynamic ray-tracing procedure in evaluating travel time approximations. For example, Ursin (1981B) has developed such approximations in the vicinity of a reference ray by use of the wavefront curvatures calculated for this ray. We are presently studying the different approximations in order to find out in which areas they are applicable for different models. This work will be presented in Gjøystdal et al (1981).

The second item is more comprehensive. It aims at applying the ray method to perform inversion of seismic data in a 3-D world. An introductory reference here would be Hubral and Krey (1980). Gjøystdal and Ursin (1981) have presented an inversion procedure using travel times and utilizing the zero and non-zero offset rays. This is an application of the generalized inverse method. Ursin (1981A) suggests the use of wavefront curvatures to perform inversion. The existence of the procedures presented in this thesis calls for extensions of these inversion methods to include even amplitude variations over the receiver area.

The last item to be mentioned is concerned with the singular regions in the ray field. Quite recently it has been suggested by Cerveny et al (1981) that the problems of the irregular regions could be overcome by use of so-called Gaussian beams. The name is due to the property of the beam's amplitude, which decreases exponentially in a Gaussian way with increasing distance from a given ray. Each beam is to be continued independently through an arbitrary inhomogeneous structure, and the complete wave field at a receiver is then obtained as an integral superposition of all Gaussian beams arriving in some neighborhood of the receiver. Also various diffraction effects are claimed to be well described in this way. A brief study of the Gaussian beam theories have given the impression that they easily could be implemented in our procedures and thus make it possible to model even the singular regions.

7. REFERENCES

Acton, F.S. (1970): Numerical Methods that Work, Harper International Edition, Harper and Row Publishers, London.

Ahlberg, J.H., E.N. Nilson and J.L. Walsh (1967): The Theory of Splines and Their Applications, Academic Press, New York.

Aki, K. and P.G. Richards (1980): Quantitative Seismology. Theory and Methods, W.H. Freeman and Company, San Francisco.

Berkhout, A.J. (1980): Seismic Migration. Imaging of Acoustic Energy by Wave Field Extrapolation, Elsevier Publishing Co., Amsterdam.

Cerveny, V. (1979A): Accuracy of theoretical seismograms, J. Geophys. 46, 135-149.

Cerveny, V. (1979B): Ray theoretical seismograms for laterally inhomogeneous structures, J. Geophys. 46, 335-342.

Cerveny, V., M.M. Popov and I. Psencik (1981): Computation of seismic wave fields in inhomogeneous media - Gaussian beam approach. Submitted to Geophys. J.R. astr. Soc.

Cerveny, V., K. Fuchs, G. Müller and J. Zahradnik (1978): Theoretical seismograms for inhomogeneous elastic media. Vopr. Dinamichenskoy Theorii Rasprostranemiya Seismicheskikch Voln., Vol. 20, G.I. Petrashen (Ed.), Leninggrad: Nauka.

Cerveny, V. and F. Hron (1980): The ray series method and dynamic ray tracing system for three dimensional inhomogeneous media. Bull. Seism. Soc. Am. 70, 47-77.

Cerveny, V., I.A. Molotkov and I. Psencik (1977): Ray Method in Seismology. Universita Karlova, Praha.

Cerveny, V. and R. Ravindra (1971): Theory of Seismic Head Waves. University of Toronto Press, Toronto.

Deschamps, G.A. (1972): Ray techniques in electromagnetics. Proc. IEEE, 60, 1022-1035.

Fuchs, K. and G. Müller (1971): Computation of synthetic seismograms with the reflectivity method and comparison with observations. Geophys. J.R. Astr. Soc., 23, 417-433.

Gjøystdal, H. (1978A): A general computer algorithm for calculating zero-value contours of a bivariate scalar function, with special application to seismic ray-tracing in complex 3-dimensional models. Technical Report No. 4/80, NTNF/NORSAR, Kjeller.

Gjøystdal, H. (1978B): Computation of seismic ray paths between given source and receiver line in a complex 3-D model. Technical Report No. 3/80, NTNF/NORSAR, Kjeller.

Gjøystdal, H. (1979): Ray tracing in complex 3-D geological models: Presented at the 49th Annual International SEG Meeting, November 5, in New Orleans.

Gjøystdal, H., J.E. Reinhardsen and B. Ursin (1981): Travel time and wavefront curvature calculations in inhomogeneous layered media with curved interfaces. Presented at the 51st Annual International SEG Meeting, October, Los Angeles.

Gjøystdal, H. and B. Ursin (1981): Inversion of reflection times in three dimensions. Geophysics 46, 972-983.

Gough, G.I. (ed.) (1980): Annual Report (1980), Institute of Earth and Planetary Physics, University of Alberta, Edmonton, Alberta.

Hubral, P. (1976): Ray tracing and 3D modelling. Presented at the 46th Annual SEG Meeting, October 28, Houston, Texas.

Hubral, P. (1979): A wavefront approach to the computing of ray amplitudes in inhomogeneous media with curved interfaces. Studia Geophy. Geodaet. Czechoslov. Akad. Ved. 23, 131-137.

Hubral, P. (1980): Wavefront curvatures in three dimensional laterally inhomogeneous media with curved interfaces. Geophysics 45, 905-913.

Hubral, P. and T. Krey (1980): Interval velocities from seismic reflection time measurements. Society of Exploration Geophysicists, Tulsa, Oklahoma. Larner, K.L. (ed.).

Hudson, J.A. (1980): The Excitation and Propagation of Elastic Waves. Cambridge Univ. Press, Cambridge.

James, G.L. (1976): Geometrical Theory of Diffraction for Electromagnetic Waves. P. Peregrinus Ltd., Stevenage.

Julian, B.R. and D. Gubbins (1977): Three dimensional seismic ray tracing. J. Geophys. 43, 95-113.

Lee, S.W. (1975): Electromagnetic reflection from a conducting surface: Geometrical optics solution. IEEE Trans. Vol AP-23, 184-191.

Popov, M.M. and I. Psencik (1978A): Ray amplitudes in inhomogeneous media with curved interfaces. Geofysicalni Sbornic, Vol 24, Academia, Prague, 111-129.

Popov, M.M. and I. Psencik (1978B): Computation of ray amplitudes in inhomogeneous media with curved interfaces. Studia Geophys. Geodaet. Ceskoslov. Akad. Ved. 22, 248-258.

Reid, W.T. (1972): Riccati Differential Equations. Academic Press, New York.

Sattlegger, J. (1965): A method of computing true velocities from expanding spread data in the case of arbitrary long spreads and arbitrary dipping plane interfaces. Geophys. Prospecting 13, 306-318.

Shah, P.M. (1973): Ray tracing in three dimensions. Geophysics 38, 600-604.

Shampine, L.F. and R.C. Allen (1973): Numerical Computing: An Introduction. Saunders, Philadelphia.

Shampine, L.F. and M.K. Gordon (1975): Computer Solution of Ordinary Differential Equations: The Initial Value Problem. W.H. Freeman and Company, San Francisco.

Sorrells, G.G., J.R. Crowley and K.F. Veith (1971): Methods for computing ray paths in complex geological structures. Bull. Seism. Soc. Am. 61, 27-53.

Taner, M.T. and F. Koehler (1969): Velocity spectra - digital computer derivation and applications of velocity functions. Geophysics 34, 859-881.

Ursin, B. (1981A): Time-to-depth migration using wavefront curvature. SINTEF Report No. STF28 A81021, Trondheim.

Ursin, B. (1981B): Quadratic wavefront and travel time approximations in inhomogeneous layered media with curved interfaces. SINTEF Report STF28 A81038, Trondheim.

Woodhouse, J.H. (1975): Aspects of high frequency wave propagation in the heterogeneous earth. Ph.D. Thesis, University of Cambridge, Cambridge.